

Non-Bayesian Activity Detection, Large-Scale Fading Coefficient Estimation, and Unsourced Random Access with a Massive MIMO Receiver

Alexander Fengler, Saeid Haghighatshoar, Peter Jung, Giuseppe Caire

Abstract

In this paper, we study the problem of user *activity detection* and large-scale fading coefficient estimation in a random access wireless uplink with a massive MIMO base station with a large number M of antennas and a large number of wireless single-antenna devices (users). We consider a block fading channel model where the M -dimensional channel vector of each user remains constant over a *coherence block* containing L signal dimensions in time-frequency. In the considered setting, the number of potential users K_{tot} is much larger than L but at each time slot only $K_a \ll K_{\text{tot}}$ of them are active. Previous results, based on compressed sensing, require that $K_a \leq L$, which is a bottleneck in massive deployment scenarios such as *Internet-of-Things* and *unsourced random access*. In this work we show that such limitation can be overcome when the number of base station antennas M is sufficiently large. More specifically, we prove that with a coherence block of dimension L and a number of antennas M such that $K_a/M = o(1)$, one can identify $K_a = O(L^2/\log^2(\frac{K_{\text{tot}}}{K_a}))$ active users, which is much larger than the previously known bounds. We also provide two algorithms. One is based on Non-Negative Least-Squares, for which the above scaling result can be rigorously proved. The other consists of a low-complexity iterative componentwise minimization of the likelihood function of the underlying problem. While for this algorithm a rigorous proof cannot be given, we analyze a constrained version of the Maximum Likelihood (ML) problem (a combinatorial optimization with exponential complexity) and find the same fundamental scaling law. Therefore, we conjecture that our low-complexity (approximated) ML algorithm also achieve the same scaling law and we demonstrate its performance by simulation. In particular, we compare the proposed methods with the (Bayesian) MMV-AMP algorithm, recently proposed for the same purpose, and show superior performance and better numerical stability (while not relying on assumptions on priors as for the Bayesian setting). Finally, we use the proposed approximated ML algorithm as the decoder for the inner code in a concatenated coding scheme for unsourced random access, where all users make use of the same codebook, and the massive MIMO base station must come up with the list of transmitted

The authors are with the Communications and Information Theory Group, Technische Universität Berlin ({fengler, saeid.haghighatshoar, peter.jung, caire}@tu-berlin.de).

A short version of this paper was presented in the 2018 IEEE International Symposium on Information Theory (ISIT) in Vail, Colorado, USA [1].

messages irrespectively of the identity of the transmitters. We show that reliable communication is possible at any E_b/N_0 provided that a sufficiently large number of base station antennas is used, and that a sum spectral efficiency in the order of $\mathcal{O}(L \log(L))$ is achievable.

Index Terms

Activity Detection, Internet of Things (IoT), Massive MIMO, Unsourced Random Access.

I. INTRODUCTION

One of the paradigms of modern machine-type communications [2] consists of a very large number of devices (here referred to as “users”) with sporadic data. Typical examples thereof are Internet-of-Things (IoT) applications, wireless sensors deployed to monitor smart infrastructure, and wearable biomedical devices [3]. In such scenarios, a Base Station (BS) should be able to collect data from a large number of devices. However, due to the sporadic nature of the data generation and communication, allocating some dedicated transmission resource to all users in the system may be extremely wasteful. We distinguish between two approaches: i) using a dedicated random access slot, the active users can be identified and the BS can then allocate transmission resources to these users. The operation is repeated over a time frame structure, such that the set of active users is tracked over time; ii) using *unsourced random access* scheme, the active users just transmit their data without any dedicated activity signaling. Interestingly, virtually any exiting cellular standard in operation today (3G, 4G-LTE, 5G New Radio) makes use of a dedicated random access channel (or slot), followed by some scheduling and resource allocation for the active users [4, 5], therefore these schemes can be seen as examples of paradigm i) above. In contrast, unsourced random access is a novel paradigm proposed in [6] and motivated by an IoT scenario where millions of cheap devices have their codebook hardwired at the moment of production, and are then disseminated into the environment. In this case, all users make use of the very same codebook and the BS must decode the list of transmitted messages irrespectively of the identity of of the active users.¹

In this paper, we are mainly interested in the problem of *Activity Detection* (AD) from a dedicated pilot slot. In the second part of the paper, we shall use the proposed AD scheme as the inner code of a concatenated coding scheme for unsourced random access.

¹If a user wishes to communicate its ID, it can send it as part of the payload. Therefore, in the paradigm of unsourced random access, if the users make use of individually different codebooks, it would be impossible for the BS to know in advance which codebook to decode since the identity of the active users is not known a priori. Hence, in this context it is in fact essential, and not just a matter of implementation costs, that all users utilize the same codebook.

AD is a fundamental challenge in massive sensor deployments and random access scenarios to be expected for IoT (see, e.g., [7–12] for some recent works) We consider a classical block-fading wireless communication channel between the users and the BS [13], where the channel coefficients remain constant over *coherence blocks* consisting of L signal dimensions in the time-frequency domain, and change randomly from block to block according to a stationary ergodic process [13]. A fundamental limitation when considering a single-antenna BS is that the required signal dimension L to identify reliably a subset of K_a active users among a set consisting of K_{tot} *potentially active* users scales as $L = O(K_a \log(\frac{K_{\text{tot}}}{K_a}))$, thus, almost linearly with K_a . To keep up with the scaling requirements in practical applications where K_a may be of the order of 10^2 and K_{tot} may be of the order of $10^4 - 10^5$, it is crucial to overcome this limitation in an efficient way that does not require devoting too many pilot dimension to AD.

In a series of recent works [11, 12, 14], AD with a massive MIMO BS with a large number M of antennas was considered and formulated as a Multiple Measurement Vector (MMV) [15–17] problem. In these works, the activity detection problem is formulated in a Bayesian way and a method based on an MMV suited version of *Approximated Message Passing* (MMV-AMP) followed by a componentwise Neyman-Pearson activity estimation by suitable thresholding is proposed. There are several issues with this problem formulation and with the proposed MMV-AMP algorithm. First, the algorithm needs to treat the Large-Scale Fading Coefficients (LSFCs)² as either as deterministic known quantities, or as random quantities whose prior distribution is known. In practice, it is not easy to individually measure the LSFC from all K_{tot} users, especially when they stay silent for a long time and move or the propagation conditions change. Also, the typical distance dependent pathloss and log-normal shadowing laws used in standard models are not quite representative of specific environments and the prior ensemble distribution would assume some spatial distribution (e.g., uniform in a cell as in [11, 14]) which is not always the case. Furthermore, the MMV-AMP algorithm can be analyzed via the state evolution method [11, 14] in the large-dimensional regime where L, K_a , and K_{tot} grow to infinity at fixed ratios $\frac{K_a}{L} \rightarrow \alpha$ and $\frac{K_{\text{tot}}}{L} \rightarrow \beta$ with $\alpha, \beta \in (0, \infty)$ while M is finite. Therefore, the regime of L linear in K_a (which we wish to beat) is somehow unavoidable in this type of analysis. Finally, it turns out that in practical scenarios where M is fairly larger than L and comparable to K_a (which are scenarios of interest in our work and in practical scenarios, where L is between 50 and 200 and M can be up to 256 antennas [18–20]), MMV-AMP is quite numerically unstable and gives pathological and unpredictable behaviors that one would like definitely to avoid in a real-world implementation.

The key to overcome the linear scaling of L with K_a consists of considering quadratic measurements,

²We refer to LSFC as the averaged received power from each user when active, up to a suitable common scaling factor. Users have different LSFCs because of different distances from the BS and large-scale effects such as log-normal shadowing.

i.e., sample covariance information. This observation was already empirically provided in [21] where a “much better than linear” regime was experimentally observed and conjectured to be achievable using LASSO applied to the sample covariance matrix of the observation. However, in [21] only a linear scaling law was proved because of the analysis of LASSO based on coherence is too weak. More recently, [22] considered the estimation of the LSFCs of unknown active users using Non-Negative Least-Squares approach applied to the same sample covariance, and proved an identifiability condition such that $K_a = O(L^2)$ such coefficients can be identified with overwhelming high probability when the pilot matrix is randomly drawn from a continuous non-degenerate distribution.

In this work, we consider a non-Bayesian approach, treating the LSFCs as deterministic unknown. We derive a new RIP (Restricted Isometry Property) for Kathri-Rao product matrices and use tools from Compressed Sensing (CS) to provide a stability analysis of the LSFC estimation and AD problem for finite SNR and finite number of antennas M . As a consequence of this analysis, we are able to show that with a coherence block of dimension L , and with a sufficient number of BS antennas M with $K_a/M = o(1)$, one can estimate the LSFC, and thus identify the activity, of up to $K_a = O(L^2 / \log^2(\frac{K_{\text{tot}}}{K_a}))$ active users among K_{tot} users. Also, in contrast with the result in [22] which applies only to the restricted case $K_{\text{tot}} = K_a = L^2$, our results apply to a wider regime where K_{tot} may be potentially much larger than L^2 and K_a , where we show that one needs to pay only a logarithmic penalty $O(\log^2(\frac{K_{\text{tot}}}{K_a}))$ for increasing the total number of users K_{tot} . This makes our proposed scheme very attractive for IoT setups, in which the number of active users K_a as well as the total number of users K_{tot} may be extremely large. The above scaling laws are obtained by analyzing the NNLS algorithm of [22].

Furthermore, we propose an improved algorithm for AD based on the Maximum-Likelihood (ML) estimation of the LSFCs of the active users. The resulting likelihood function minimization is a non-convex problem, that we solve (approximately) by iterative componentwise minimization. This yields an iterative scheme based on rank-1 updates whose complexity is comparable to that of NNLS and MMV-AMP. Extensive numerical simulations show that our proposed ML algorithm is superior to NNLS and to MMV-AMP in any regime, and does not suffer from the ill-conditioned behavior of MMV-AMP for the case of large M .

While it is not possible to directly analyze our ML approach, we consider a constrained version of the ML scheme that lends itself to analysis. While the constrained ML yields a combinatorial minimization with exponential complexity and therefore is not useful in practice, we can show that the scaling law for successful detection of the activity pattern of the constrained ML scheme is the same as what found for NNLS. Therefore, we conjecture that our proposed (low-complexity) ML algorithm achieves the same scaling law. We would like to mention that an analysis of the constrained ML estimator was recently

presented in [23]. However, the results in [23] are based on a RIP result that was first claimed and then withdrawn by the same authors [24]. Hence, our result based on a new RIP and a few consequent modifications which we duly prove, essentially rigorizes the analysis presented in [23].

Finally, we focus on unsourced random access with a massive MIMO BS. It is evident that the AD problem and the random access problem are related. In fact, one can immediately obtain a random access scheme from an AD scheme as follows: assign to each user a unique set of pilot signature sequences (codewords), such that a user, when active, will transmit the signature corresponding to its information message. Since the number of pilot signatures is $K_{\text{tot}} \gg K_a$, this scheme involves only an expansion of the number of total users from K_{tot} to $K'_{\text{tot}} = K_{\text{tot}}2^B$ where B is the number of per-message information bits. This idea was recently presented in [9], where the MMV-AMP detector of [11, 14, 17] was used at the receiver side. While conceptually simple, this approach has two major drawbacks: 1) even for relatively small information packets (e.g., $B = 100$ bits), the dimension of the pilot matrix is too large for practical computational algorithms; 2) each user has a different set of pilot sequences, and therefore the scheme is not compliant with the basic assumption of unsourced random access, that users have all the same codebook.

In contrast, we present a novel scheme, build upon the concatenated coding approach of [25], that does not incur in the large dimension problem and is independent of the number of “inactive” users. In our scheme, the message of B bits of each user is split into a sequence of submessages of potentially different lengths. These submessages are encoded via a tree code (the same for each user), such that the encoded blocks have the same length of J bits. Then, each user transmits its sequence of J -bits blocks in consecutive blocks of L dimensions, using the same $L \times 2^J$ pilot matrix (where blocks are encoded in the matrix columns). The inner detector perform our ML activity detection scheme and for each slot recovers the set of active columns of the pilot matrix. These are passed to the outer tree code, which recovers each user message by “stitching together” the sequence of submessages. We show that an arbitrary small probability of error is achievable at any E_b/N_0 provided that a sufficiently large number of base station antennas is used, and that the sum spectral efficiency can grow as $\mathcal{O}(L \log(L))$. This can be achieved in a completely non-coherent way, i.e. it is at no point necessary to estimate the channel matrix (small-scale fading coefficients). These are important properties to enable easily deployable, low-latency, energy efficient communication in an IoT setting.

A. Notation

We represent scalar constants by non-boldface letters (e.g., x or X), sets by calligraphic letters (e.g., \mathcal{X}), vectors by boldface small letters (e.g., \mathbf{x}), and matrices by boldface capital letters (e.g., \mathbf{X}). We denote the i -th row and the j -th column of a matrix \mathbf{X} with the row-vector $\mathbf{X}_{i,:}$ and the column-vector $\mathbf{X}_{:,j}$

respectively. We denote a diagonal matrix with elements (s_1, s_2, \dots, s_k) by $\text{diag}(s_1, \dots, s_k)$. We denote the vectorization operator by $\text{vec}(\cdot)$. We denote the ℓ_p -norm of a vector \mathbf{x} and the Frobenius norm of a matrix \mathbf{X} by $\|\mathbf{x}\|_p$ and $\|\mathbf{X}\|_p$ resp. $\|\mathbf{x}\|_0 := |\{i : x_i \neq 0\}|$ denotes the number of non-zero entries of a vector \mathbf{x} . The operator norm of a matrix \mathbf{X} is denoted by $\|\mathbf{X}\|_{op}$. The $k \times k$ identity matrix is represented by \mathbf{I}_k . For an integer $k > 0$, we use the shorthand notation $[k]$ for $\{1, 2, \dots, k\}$. We use superscripts $(\cdot)^\top$ and $(\cdot)^H$ for transpose and Hermitian transpose. \odot denotes the elementwise product of vectors or matrices of the same size. $\langle \mathbf{x}, \mathbf{y} \rangle := \mathbf{x}^H \mathbf{y}$ denotes the Euclidean scalar product between two vectors. We define universal constants to be numbers, which are independent of all system parameters. Such constants are typically denoted by c, C, c', c_0, c_1 etc., and different universal constants may be denoted by the same letter. $\log(x)$ denotes the natural logarithm of x .

II. PROBLEM FORMULATION

A. Signal Model

We consider a classical block-fading wireless channel between each user and the BS where the channel coefficients remain constant over coherence blocks consisting of L signal dimensions in time-frequency [13], and change from block to block according to some stationary and ergodic fading process. In general, the BS devotes some time-frequency slots to AD, i.e., to the purpose of identifying the active users who want to request some transmission resource. Such slots are generally non-adjacent in the time-frequency domain, since they are multiplexed with other slots, dedicated to data transmission of the already connected users. Since typically the number of signal dimensions per AD slot is not larger than one coherence block, without loss of generality we assume that each AD slot consists of L signal dimensions and coincides with a coherence block. We denote the set of all potential users (which may or may not be active) as \mathcal{K}_{tot} , of size $K_{\text{tot}} := |\mathcal{K}_{\text{tot}}|$. Each user $k \in \mathcal{K}_{\text{tot}}$ is given a user-specific and a priori known pilot sequence. The pilot sequence of user k is denoted as $\mathbf{a}_k = (a_{k,1}, \dots, a_{k,L})^\top \in \mathbb{C}^L$. If user k is active, it transmits the components of \mathbf{a}_k in the AD slot of L signal dimensions. Denoting by \mathbf{h}_k the M -dim channel vector (small-scale fading coefficients) of the user $k \in \mathcal{K}_{\text{tot}}$ to M antennas at the BS, we can write the received signal at the BS over the AD slot as

$$\mathbf{y}[i] = \sum_{k \in \mathcal{K}_{\text{tot}}} b_k \sqrt{g_k} a_{k,i} \mathbf{h}_k + \mathbf{z}[i], \quad i \in [L], \quad (1)$$

where $[L] := \{1, \dots, L\}$, $g_k \in \mathbb{R}_+$ denotes the LSFC (channel strength) of the user $k \in \mathcal{K}_{\text{tot}}$, $b_k \in \{0, 1\}$ is a binary variable with $b_k = 1$ for active and $b_k = 0$ for inactive users and $\mathbf{z}[i] \sim \mathcal{CN}(0, \sigma^2 \mathbf{I}_M)$ denotes the additive white Gaussian noise (AWGN) at the i -th signal dimension.

Denoting by $\mathbf{Y} = [\mathbf{y}[1], \dots, \mathbf{y}[L]]^\top$ the $L \times M$ received signal over L signal dimensions and M BS antennas, we can write (1) more compactly as

$$\mathbf{Y} = \mathbf{A}\mathbf{\Gamma}^{\frac{1}{2}}\mathbf{H} + \mathbf{Z}, \quad (2)$$

where $\mathbf{A} = [\mathbf{a}_1, \dots, \mathbf{a}_{K_{\text{tot}}}]$ denotes the $L \times K_{\text{tot}}$ matrix of pilot sequences of the users in \mathcal{K}_{tot} , where $\mathbf{\Gamma} = \mathbf{B} \odot \mathbf{G}$ where \mathbf{G} is a $K_{\text{tot}} \times K_{\text{tot}}$ diagonal matrix consisting of the LSFCs $(g_1, \dots, g_{K_{\text{tot}}})^\top$ and where \mathbf{B} is a $K_{\text{tot}} \times K_{\text{tot}}$ diagonal matrix consisting of the binary activity patterns $(b_1, \dots, b_{K_{\text{tot}}})^\top$ of the users, and where $\mathbf{H} = [\mathbf{h}_1, \dots, \mathbf{h}_{K_{\text{tot}}}]^\top$ denotes $K_{\text{tot}} \times M$ matrix containing the M -dim normalized channel vectors of the users.

In line with the classical massive MIMO setting [26], we assume for simplicity an independent Rayleigh fading model, such that the channel vectors $\{\mathbf{h}_k : k \in \mathcal{K}_{\text{tot}}\}$ are independent from each other and are spatially white (i.e., uncorrelated along the antennas), that is, $\mathbf{h}_k \sim \mathcal{CN}(0, \mathbf{I}_M)$. We would like to mention here that massive MIMO has been now investigated under many more realistic propagation conditions involving antenna correlation and partial Line-of-Sight Rician fading [27, 28]. Nevertheless, for consistency with respect to [11, 14], where this assumption is made, and for the sake of isolating the fundamental aspects of the problem without additional model complication, we stick to the simple i.i.d. Rayleigh fading model. A thorough study of the effect of different small-scale fading statistics (e.g., introducing correlation across the antennas for each user channel) is left for future work.

The user pilots are normalized to unit energy per symbol, i.e., $\|\mathbf{a}_k\|_2^2 = L$. Then, the average SNR of a generic active user $k \in \mathcal{K}_{\text{tot}}$ over L pilot dimensions is given by

$$\text{snr}_k = \frac{\|\mathbf{a}_k\|_2^2 \gamma_k \mathbb{E}[\|\mathbf{h}_k\|_2^2]}{\mathbb{E}[\|\mathbf{Z}\|_F^2]} = \frac{L\gamma_k M}{LM\sigma^2} = \frac{\gamma_k}{\sigma^2} = \frac{g_k}{\sigma^2}, \quad (3)$$

where $\gamma_k = b_k g_k = g_k$ ($b_k = 1$ for active users) is the k -th diagonal element of $\mathbf{\Gamma}$. We call the vector $\boldsymbol{\gamma} = (\gamma_1, \dots, \gamma_{K_{\text{tot}}})^\top$ or equivalently the diagonal matrix $\mathbf{\Gamma} = \text{diag}(\boldsymbol{\gamma})$ the ‘‘active LSFC pattern’’ of the users in \mathcal{K}_{tot} . We denote by $\mathcal{K}_a \subseteq \mathcal{K}_{\text{tot}}$ the subset of active users in the current AD slot, with size $K_a := |\mathcal{K}_a|$. Thus, $\boldsymbol{\gamma}$ is a non-negative sparse vector with only K_a nonzero elements. The goal of AD is to identify the subset of active users \mathcal{K}_a or a subset thereof consisting of users with sufficiently strong channels $\mathcal{K}_a(\nu) := \{k \in \mathcal{K}_{\text{tot}} : \gamma_k > \nu\sigma^2\}$, for a pre-specified threshold $\nu > 0$, from the noisy observations as in (2). As a side goal, we wish also to estimate the LSFCs γ_k of the active users (at least those above threshold). This information may be useful in practice to accomplish tasks such as user-BS association, user scheduling, and possibly other high-level network optimization tasks where the knowledge of the user channel strength is relevant.

Since we assume that the channel vectors are spatially white and Gaussian, the columns of \mathbf{Y} in (2)

are i.i.d. Gaussian vectors with $\mathbf{Y}_{:,i} \sim \mathcal{CN}(0, \boldsymbol{\Sigma}_{\mathbf{y}})$ where

$$\boldsymbol{\Sigma}_{\mathbf{y}} = \mathbf{A}\boldsymbol{\Gamma}\mathbf{A}^H + \sigma^2\mathbf{I}_L = \sum_{k=1}^{K_{\text{tot}}} \gamma_k \mathbf{a}_k \mathbf{a}_k^H + \sigma^2\mathbf{I}_L \quad (4)$$

denotes the covariance matrix, which is common among all the columns $\mathbf{Y}_{:,i}$, $i \in [M]$. We also define the empirical/sample covariance of the columns of the observation \mathbf{Y} in (2) as

$$\widehat{\boldsymbol{\Sigma}}_{\mathbf{y}} = \frac{1}{M} \mathbf{Y}\mathbf{Y}^H = \frac{1}{M} \sum_{i=1}^M \mathbf{Y}_{:,i} \mathbf{Y}_{:,i}^H. \quad (5)$$

III. PROPOSED ALGORITHMS FOR ACTIVITY DETECTION

In this section, we propose two algorithms for AD and LSFC estimation.

A. Maximum Likelihood Estimation

We first consider the Maximum Likelihood (ML) estimator of $\boldsymbol{\gamma}$ by making explicit use of Gaussianity of the users channel vectors. We introduce the log-likelihood cost function

$$f(\boldsymbol{\gamma}) := -\frac{1}{M} \log p(\mathbf{Y}|\boldsymbol{\gamma}) \stackrel{(a)}{=} -\frac{1}{M} \sum_{i=1}^M \log p(\mathbf{Y}_{:,i}|\boldsymbol{\gamma}) \quad (6)$$

$$= \log |\mathbf{A}\boldsymbol{\Gamma}\mathbf{A}^H + \sigma^2\mathbf{I}_L| + \text{tr} \left(\left(\mathbf{A}\boldsymbol{\Gamma}\mathbf{A}^H + \sigma^2\mathbf{I}_L \right)^{-1} \widehat{\boldsymbol{\Sigma}}_{\mathbf{y}} \right), \quad (7)$$

where (a) follows from the fact that the columns of \mathbf{Y} are i.i.d. (due to the spatially white user channel vectors), and where $\widehat{\boldsymbol{\Sigma}}_{\mathbf{y}}$ denotes the sample covariance matrix of the columns of \mathbf{Y} as in (5). Note that for spatially white channel vectors considered here, $\widehat{\boldsymbol{\Sigma}}_{\mathbf{y}} \rightarrow \boldsymbol{\Sigma}_{\mathbf{y}}$ as the number of antennas $M \rightarrow \infty$. It is apparent that the likelihood function $p(\mathbf{Y}|\boldsymbol{\gamma})$ depends on \mathbf{Y} only through the covariance matrix $\widehat{\boldsymbol{\Sigma}}_{\mathbf{y}}$. Therefore, $\widehat{\boldsymbol{\Sigma}}_{\mathbf{y}}$ is a *sufficient statistic* for the estimation of $\boldsymbol{\gamma}$ or any function thereof. Especially in a Massive MIMO scenario, where $M > L$, the use of the covariance matrix $\widehat{\boldsymbol{\Sigma}}_{\mathbf{y}} \in \mathbb{C}^{L \times L}$ instead of the raw measurements $\mathbf{Y} \in \mathbb{C}^{M \times L}$ results in a significant dimensionality reduction. Now let us focus on the ML cost function in (7). Assuming the number of active users K_a is known, the *constrained ML estimator* of $\boldsymbol{\gamma}$ is given by

$$\boldsymbol{\gamma}_{\text{c-ML}}^* = \arg \min_{\boldsymbol{\gamma} \in \Theta_{K_a}^+} f(\boldsymbol{\gamma}). \quad (8)$$

where the constraint set $\Theta_{K_a}^+ = \{\boldsymbol{\gamma} \in \mathbb{R}_+^{K_{\text{tot}}} : \|\boldsymbol{\gamma}\|_0 \leq K_a\}$ is the (non-convex) set of non-negative K_a -sparse vectors. There are two problems with this estimator: 1) K_a is generally not known a priori, and 2) the minimization in (8) is combinatorial and has exponential complexity in K_{tot} , which can be very large. Therefore, this ML estimator has no practical value. Nevertheless, its performance yields a useful bound

to the performance of other “relaxed” versions of ML estimation. In particular, we are interested in the *relaxed ML estimator* of γ given by

$$\gamma_{\text{r-ML}}^* = \arg \min_{\gamma \in \mathbb{R}_+^{K_{\text{tot}}}} f(\gamma). \quad (9)$$

It is not difficult to check that $f(\gamma)$ in (7) is the sum of a concave function and a convex function, so also the problem in (9) is not convex in general. Notice also that the estimator in (9) does not require any prior knowledge of K_a .

In the following, for the sake of analysis, we shall denote the true vector of LSFCs as \mathbf{g}° and the true activity pattern as \mathbf{b}° . Next, we consider the performance of the constrained ML estimator (8). The idea of the proof is based on [23], which was relying on a RIP result [24] which was then withdrawn since the proof had a flaw. In Appendix A we give a complete and streamlined proof for the case, where the true vector of LSFCs \mathbf{g}° is known at the receiver and all entries satisfy $g_k^\circ \in [g_{\min}, g_{\max}]$. Therefore, the goal consist of estimating the activity pattern \mathbf{b}° and the active LSFC pattern is eventually given by $\gamma_{\text{c-ML}}^* = \mathbf{b}^* \odot \mathbf{g}^\circ$, where \mathbf{b}^* is the estimate of \mathbf{b}° . We hasten to say that our proof technique extends easily also to the case where \mathbf{g}° is unknown, provided that the per-component upper and lower bounds g_{\min} and g_{\max} are known, using the arguments of [23]. We have omitted this general case for the sake of brevity, since it requires a few more technicalities which can be found in [23].

For the case at hand, we define the constrained ML estimator of the activity pattern $\mathbf{b}^\circ \in \{0, 1\}^{K_{\text{tot}}}$ as

$$\mathbf{b}^* := \arg \min_{\mathbf{b} \in \Theta_{K_a}} f(\mathbf{b} \odot \mathbf{g}^\circ), \quad (10)$$

with $f(\cdot)$ as defined in (6) and $\Theta_{K_a} = \{\mathbf{b} \in \{0, 1\}^{K_{\text{tot}}} : \sum b_k = K_a\}$, the set of binary K_a -sparse vectors. We have the following result:

Theorem 1: Let the LSFCs be such that for all k it holds that $g_{\min} \leq g_k \leq g_{\max}$. Let $\mathbf{A} \in \mathbb{C}^{L \times K_{\text{tot}}}$, be the pilot matrix with columns drawn uniformly i.i.d. from the sphere of radius \sqrt{L} and let $K_{\text{tot}} > L^2$. The estimate \mathbf{b}^* , defined in (10), satisfies $\mathbf{b}^* = \mathbf{b}^\circ$ with probability exceeding $1 - 2\epsilon - \exp(-CL)$, provided that

$$K_a \leq c \frac{L^2}{\log^2(eK_{\text{tot}}/L^2)}, \quad (11)$$

and

$$M \geq \frac{4}{1 - \delta} \left(\frac{C' g_{\max} \left(2 \log\left(\frac{eK_{\text{tot}}}{2K_a}\right) + \frac{\log(2/\epsilon)}{\max\{K_a, L\}} \right) \max\left\{1, \frac{K_a}{L}\right\} + \frac{\sigma^2}{L}}{g_{\min}} \right)^2 \log \left(3eK_{\text{tot}}K_a \frac{1 + \epsilon}{\epsilon} \right) \quad (12)$$

where $\delta < 1$ and $c, C, C' > 0$ are universal constants. □

Proof: See Appendix A ■

Simple algebra (omitted for the sake of brevity) shows the following:

Corollary 1: Let \mathbf{A} be as above and let $M, K_a, L \rightarrow \infty$, then it is possible to choose

$$K_a = \mathcal{O}(L^2 / \log^2(K_{\text{tot}}/L^2)) \quad (13)$$

and

$$M = \mathcal{O}\left(K_a(g_{\text{max}}/g_{\text{min}})^2 \log^2(K_{\text{tot}}/K_a) \log(K_{\text{tot}}K_a)\right) \quad (14)$$

such that the estimation error of the ML estimator (10) vanishes. \square

As said, the minimization in (8) or (10) is in general computationally unfeasible (beyond the problem of not knowing K_a). Next, we consider the relaxed ML estimator (9) and show that it can be computed using a low complexity iterative algorithm based on rank-1 updates. While this algorithm is not known to converge to the exact minimum of the ML cost function, empirical evidence suggests it converges very well. The algorithm proceeds as follows:

For each coordinate $k \in [K_{\text{tot}}]$, define the scalar function $f_k(d) = f(\boldsymbol{\gamma} + d\mathbf{e}_k)$ where $f(\boldsymbol{\gamma})$ is the likelihood function (7) and \mathbf{e}_k denotes the k -th canonical basis vector with a single 1 at its k -th coordinate and zero elsewhere. Setting $\boldsymbol{\Sigma} = \boldsymbol{\Sigma}(\boldsymbol{\gamma}) = \mathbf{A}\boldsymbol{\Gamma}\mathbf{A}^H + \sigma^2\mathbf{I}_L$ where $\boldsymbol{\Gamma} = \text{diag}(\boldsymbol{\gamma})$ and applying the well-known Sherman-Morrison rank-1 update identity [29] we obtain that

$$(\boldsymbol{\Sigma} + d\mathbf{a}_k\mathbf{a}_k^H)^{-1} = \boldsymbol{\Sigma}^{-1} - \frac{d\boldsymbol{\Sigma}^{-1}\mathbf{a}_k\mathbf{a}_k^H\boldsymbol{\Sigma}^{-1}}{1 + d\mathbf{a}_k^H\boldsymbol{\Sigma}^{-1}\mathbf{a}_k}. \quad (15)$$

Using (15) and applying the well-known determinant identity

$$|\boldsymbol{\Sigma} + d\mathbf{a}_k\mathbf{a}_k^H| = (1 + d\mathbf{a}_k^H\boldsymbol{\Sigma}^{-1}\mathbf{a}_k)|\boldsymbol{\Sigma}|, \quad (16)$$

we can simplify $f_k(d)$ as follows

$$f_k(d) = c + \log(1 + d\mathbf{a}_k^H\boldsymbol{\Sigma}^{-1}\mathbf{a}_k) - \frac{\mathbf{a}_k^H\boldsymbol{\Sigma}^{-1}\widehat{\boldsymbol{\Sigma}}_y\boldsymbol{\Sigma}^{-1}\mathbf{a}_k}{1 + d\mathbf{a}_k^H\boldsymbol{\Sigma}^{-1}\mathbf{a}_k}d \quad (17)$$

where $c = \log|\boldsymbol{\Sigma}| + \text{tr}(\boldsymbol{\Sigma}^{-1}\widehat{\boldsymbol{\Sigma}}_y)$ is a constant term independent of d . Note that from (17), $f_k(d)$ is well-defined only when $d > d_0 := -\frac{1}{\mathbf{a}_k^H\boldsymbol{\Sigma}^{-1}\mathbf{a}_k}$. Taking the derivative of $f_k(d)$ yields

$$f'_k(d) = \frac{\mathbf{a}_k^H\boldsymbol{\Sigma}^{-1}\mathbf{a}_k}{1 + d\mathbf{a}_k^H\boldsymbol{\Sigma}^{-1}\mathbf{a}_k} - \frac{\mathbf{a}_k^H\boldsymbol{\Sigma}^{-1}\widehat{\boldsymbol{\Sigma}}_y\boldsymbol{\Sigma}^{-1}\mathbf{a}_k}{(1 + d\mathbf{a}_k^H\boldsymbol{\Sigma}^{-1}\mathbf{a}_k)^2}. \quad (18)$$

The only solution of $f'_k(d) = 0$ is given by

$$d^* = \frac{\mathbf{a}_k^H\boldsymbol{\Sigma}^{-1}\widehat{\boldsymbol{\Sigma}}_y\boldsymbol{\Sigma}^{-1}\mathbf{a}_k - \mathbf{a}_k^H\boldsymbol{\Sigma}^{-1}\mathbf{a}_k}{(\mathbf{a}_k^H\boldsymbol{\Sigma}^{-1}\mathbf{a}_k)^2}. \quad (19)$$

Note that $d^* \geq d_0 = -\frac{1}{\mathbf{a}_k^H\boldsymbol{\Sigma}^{-1}\mathbf{a}_k}$, thus, one can check from (17) that f_k is indeed well-defined at $d = d^*$. Moreover, we can check from (17) that $\lim_{\epsilon \rightarrow 0^+} f_k(d_0 + \epsilon) = \lim_{d \rightarrow \infty} f_k(d) = \infty$, thus, $d = d^*$ must be the global minimum of $f_k(d)$ in (d_0, ∞) . Note that since after the update we have $\gamma_k \leftarrow \gamma_k + d$, to

preserve the positivity of γ_k , the optimal update step d is in fact given by $\max\{d^*, -\gamma_k\}$ as illustrated in Algorithm 1.

The exact characterization of the performance of this algorithm remains at the moment an open problem. A way to find the asymptotic distribution of $\gamma_{\text{r-ML}}^*$ was recently proposed [30]. Of course, this applies to the true solution of (9) and not to the outcome of our proposed low-complexity iterative algorithm. Furthermore, this analysis method holds only for the overdetermined case $K_{\text{tot}} \leq L^2$, i.e. when the matrix (23) has more rows than columns, while empirically we observed excellent performance also for the underdetermined case where $K_{\text{tot}} > L^2$ (which is an assumption required by Theorem 1).

B. Non-Negative Least Squares

Let us first note some property of the log-likelihood cost function (6). Define

$$\Sigma(\boldsymbol{\gamma}) := \mathbf{A}\boldsymbol{\Gamma}\mathbf{A}^H + \sigma^2\mathbf{I}_L \quad (20)$$

and let

$$\phi(\boldsymbol{\Sigma}) := -\log |\boldsymbol{\Sigma}| + \text{tr}(\boldsymbol{\Sigma}\widehat{\boldsymbol{\Sigma}}_{\mathbf{y}}). \quad (21)$$

Since $\Sigma(\boldsymbol{\gamma})$ is positive definite for every non-negative vector $\boldsymbol{\gamma}$, it is also invertible and the log-likelihood cost function can be expressed as $f(\boldsymbol{\gamma}) = \phi((\boldsymbol{\Sigma}(\boldsymbol{\gamma}))^{-1})$. Now $\phi : \mathbb{C}^{L \times L} \rightarrow \mathbb{R}$ is *strictly* convex. Hence, it has a unique minimal value over a convex set. The special structure of the log-likelihood cost function suggests the following heuristic: first, find the matrix $\arg \min_{\boldsymbol{\Xi} \in \mathcal{S}_L^+} \phi(\boldsymbol{\Xi})$, a simple calculation shows that it is given by the inverse of the empirical covariance matrix $\widehat{\boldsymbol{\Sigma}}_{\mathbf{y}}$; then, find the estimate of $\boldsymbol{\gamma}$ as

$$\boldsymbol{\gamma}^* = \arg \min_{\boldsymbol{\gamma} \in \mathbb{R}_+^K} \|\boldsymbol{\Sigma}(\boldsymbol{\gamma}) - \widehat{\boldsymbol{\Sigma}}_{\mathbf{y}}\|_F^2. \quad (22)$$

This approach will be justified later, since we will proof a non-asymptotic bound on the recovery error $\|\boldsymbol{\gamma}^* - \boldsymbol{\gamma}^\circ\|_1$, which shows that, under certain conditions, the error vanishes in the limit $M \rightarrow \infty$. Let us introduce the matrix $\mathbb{A} \in \mathbb{C}^{L^2 \times K_{\text{tot}}}$, whose k -th column is defined by:

$$\mathbb{A}_{:,k} := \text{vec}(\mathbf{a}_k \mathbf{a}_k^H). \quad (23)$$

and let $\mathbf{w} = \text{vec}(\widehat{\boldsymbol{\Sigma}}_{\mathbf{y}} - \sigma^2\mathbf{I}_L)$ denote the $L^2 \times 1$ vector obtained by stacking the columns of $\widehat{\boldsymbol{\Sigma}}_{\mathbf{y}} - \sigma^2\mathbf{I}_L$. Then, we can write (22) in the convenient form

$$\boldsymbol{\gamma}^* = \arg \min_{\boldsymbol{\gamma} \in \mathbb{R}_+^K} \|\mathbb{A}\boldsymbol{\gamma} - \mathbf{w}\|_2^2, \quad (24)$$

as a linear *least squares* problem with non-negativity constraint, known as *non-negative least squares* (NNLS). Such an algorithm was proposed for the activity detection problem in [22].

NNLS has a special property, as discussed for example in [31] and referred to as the \mathcal{M}^+ -criterion in [32], which makes it particularly suitable for recovering sparse vectors: If the row span of \mathbb{A} intersects

the positive orthant, NNLS implicitly also performs ℓ_1 -regularization. Because of these features, NNLS has recently gained interest in many applications in signal processing [33], compressed sensing [32], and machine learning. In our case the \mathcal{M}^+ -criterion is fulfilled in an optimally-conditioned manner and allows us to establish the following result:

Theorem 2: Let $\mathbf{A} \in \mathbb{C}^{L \times K_{\text{tot}}}$, be the pilot matrix with columns drawn uniformly i.i.d. from the sphere of radius \sqrt{L} . There exist universal constants $c_i > 0$, $i = 1, \dots, 5$, depending only on some common parameter, but not on the system parameters, (see the proof in Appendix B for details) such that, if

$$s \leq c_1 \frac{L^2}{\log^2(eK_{\text{tot}}/L^2)}, \quad (25)$$

then with probability exceeding $1 - \exp(-c_5 L)$ the following holds: For all s -sparse activity pattern vectors γ° , the solution γ^* of (24) fulfills for $1 \leq p \leq 2$ the bound:

$$\|\gamma^\circ - \gamma^*\|_p \leq \frac{c_2}{s^{1-\frac{1}{p}}} \sigma_s(\gamma^\circ)_1 + \frac{c_3}{s^{\frac{1}{2}-\frac{1}{p}}} \left(\frac{\sqrt{L}}{\sqrt{s}} + c_4 \right) \frac{\|\mathbf{d}\|_2}{L}, \quad (26)$$

where $\sigma_s(\gamma^\circ)_1$ denotes the ℓ_1 -norm of γ° after removing its s largest components and where

$$\mathbf{d} = \text{vec} \left(\widehat{\Sigma}_{\mathbf{y}} - \sum_{k=1}^{K_{\text{tot}}} \gamma_k^\circ \mathbf{a}_k \mathbf{a}_k^H - \sigma^2 \mathbf{I}_L \right). \quad (27)$$

□

The proof is based on a combination of the NNLS results of [32] and an extension of RIP-results for the heavy-tailed column-independent model [34, 35]. The common parameter on that the constants c_i depend is the RIP constant of a properly centered version of \mathbb{A} , defined in (23). We state this dependence explicitly to emphasize that Theorem 2 holds also for more general random models for \mathbf{A} , for which \mathbb{A} has the RIP. Then the constants c_2, c_3, c_4 can be computed explicitly (see Appendix B) depending on the RIP constant of the other matrix model. The probability term $1 - \exp(-c_5 L)$ is precisely the probability that the centered version of the random matrix \mathbb{A} has the RIP. The result is uniform meaning that with high probability (on a draw of \mathbf{A}) it holds *for all* γ° . For $s = K_a = \|\gamma^\circ\|_0$ it implies (up to the $\|\mathbf{d}\|_2$ -term) exact recovery since in this case $\sigma_s(\gamma^\circ)_1 = 0$. A relevant extension of this result to the case $p \rightarrow \infty$ would be important but, in this generality, it is not known whether one can hope for a linear scaling in s (see here for example [36, Theorem 3.2]). Nonetheless, since $\|\cdot\|_\infty \leq \|\cdot\|_p$ our result (26) also implies an estimate for the communication relevant ℓ_∞ -case but with sub-optimal scaling (we will discuss this below). Furthermore improvements for this particular case may be possible in the non-uniform or averaged case, as it has been investigated for the sub-Gaussian case in [31].

The analysis of the term $\|\mathbf{d}\|_2$ given in Appendix C shows that

$$\mathbb{E}[\|\mathbf{d}\|_2] = \frac{L}{\sqrt{M}} (\|\gamma^\circ\|_1 + \sigma^2) \quad (28)$$

with a deviation tail distribution satisfying

$$\mathbb{P}(\|\mathbf{d}\|_2 > \sqrt{\alpha_\epsilon} \mathbb{E}[\|\mathbf{d}\|_2]) \leq \epsilon \quad (29)$$

for

$$\alpha_\epsilon = c \log((eL)^2/\epsilon) \quad (30)$$

with some universal constant $c > 0$. Setting $s = K_a$ in Theorem 2 (yielding $\sigma_s(\gamma^\circ) = 0$), for $p = 1$ we get the following:

Corollary 2: With the assumptions as in Theorem 2, the following holds: For any K_a -sparse γ° the NNLS estimate γ^* fulfills:

$$\frac{\|\gamma^\circ - \gamma^*\|_1}{\|\gamma^\circ\|_1} \leq c_3 \left(\sqrt{L} + c_4 \sqrt{K_a} \right) \frac{1 + \frac{\sigma^2}{\|\gamma^\circ\|_1}}{\sqrt{M/\alpha_\epsilon}} \quad (31)$$

with probability at least $1 - \epsilon - \exp(-c_5 L)$, where c_3, c_4, c_5 are the same constants as in Theorem 2, provided that

$$K_a \log^2 \left(\frac{K_{\text{tot}}}{K_a} \right) = \mathcal{O}(L^2). \quad (32)$$

□

Using the well-known inequality $\|\gamma^\circ\|_1 \leq \sqrt{K_a} \|\gamma^\circ\|_2$, Theorem 2 for the case $p = 2$ gives:

Corollary 3: Under the same conditions as in Corollary 2

$$\frac{\|\gamma^\circ - \gamma^*\|_2}{\|\gamma^\circ\|_2} \leq c_3 \left(\sqrt{L} + c_4 \sqrt{K_a} \right) \frac{\left(1 + \frac{\sigma^2}{\sqrt{K_a} \|\gamma^\circ\|_2} \right)}{\sqrt{M/\alpha_\epsilon}} \quad (33)$$

holds with probability at least $1 - \epsilon - \exp(-c_5 L)$ where c_3, c_4, c_5 are the same constants as in Theorem 2 provided that (32) holds. □

In conclusion, the following scaling law in order to achieve a vanishing estimation error

Corollary 4: Let $M, K_a, L \rightarrow \infty$ with fixed ratios $K_a/L^2 \log^2(eK_{\text{tot}}/L^2) = c_1$ and $M = K_a^\kappa$ for $\kappa > 1$, where c_1 is the constant from (25), then for $p = 1, 2$ it holds with probability 1 that

$$\lim_{M \rightarrow \infty} \frac{\|\gamma^\circ - \gamma^*\|_p}{\|\gamma^\circ\|_p} = 0. \quad (34)$$

□

This shows that the NNLS estimator (22) can identify up to $O(L^2)$ active users by paying only a poly-logarithmic penalty $O(\log^2(\frac{K_{\text{tot}}}{K_a}))$ for increasing the number of potential users K_{tot} . Note that this scaling is up to poly-logarithmic factors, the same as that of the (uncomputable) restricted ML estimator, see Corollary 1. This is a very appealing property in practical IoT setups where, as already mentioned in the introduction, K_{tot} may be very large.

C. Iterative Algorithms

Finding the ML estimate γ^* in (9) or the NNLS estimate (22) requires the optimization of a function over the positive orthant $\mathbb{R}_+^{K_{\text{tot}}}$. In Section III-A we have derived the componentwise minimization condition (19) of the log-likelihood cost function. Starting from an initial point γ , at each step of the algorithm we minimize $f(\gamma)$ with respect to only one of its arguments γ_k according to (19). We refer to the resulting scheme as an *iterative componentwise minimization algorithm*. Hopefully, this will converge to the solution of (9). Variants of the algorithm may differ in the way the initial point is chosen and in the way the components are chosen for update. We can also include the noise variance σ^2 as an additional optimization parameter and estimate it along γ .

The same iterative componentwise minimization approach can be used to solve (iteratively) the NNLS problem (22). Of course, the component update step is different in the case of ML and in the case of NNLS. We omit the derivation of the NNLS component update since it consists of a straightforward differentiation operation. Since NNLS is convex, in this case the componentwise minimization algorithm is guaranteed to converge to the solution of the NNLS problem (22). Given the analogy of the two iterative componentwise minimization algorithms for ML and for NNLS, we summarize them in a unified manner in Algorithm 1.

1) ML and NNLS with Knowledge of the LSFCs

Since the ML and NNLS algorithms are non-Bayesian in nature, they work well without any a-priori information on the LSFCs. If \mathbf{g}° (true values of the LSFCs of all users, active and not) is known, the algorithms can be slightly improved by projecting each k -th coordinate update on the interval $[0, g_k^\circ]$ (see step 8) in Algorithm 1. In this case the thresholding step can be improved by choosing the thresholds relative to the channel strength $\hat{\mathcal{A}}_{\mathbf{g}^\circ} = \{i : \hat{\gamma}_i > \theta g_k^\circ\}$.

IV. EMPIRICAL COMPARISON: ML, NNLS AND MMV-AMP

In this section, we compare the performance of ML, NNLS and MMV-AMP via numerical simulations.

A. Simulation Setting and Performance Criteria

We assume that the output of each algorithm is an estimate γ^* of the active LSFC pattern of the users. We use the relative ℓ_1 norm of the difference $\|\gamma^* - \gamma^\circ\|_1 / \|\gamma^\circ\|_1$ as a measure of estimate quality. The ℓ_1 norm is the natural choice here, since the coefficients γ_i represent signal received, i.e., they are related to the square of the signal amplitudes. Therefore, a more traditional ‘‘Square Error’’ (ℓ_2 norm), related to the 4th power of the signal amplitude, does not really have any relevant physical meaning for the underlying

Algorithm 1 Activity Detection via Coordinate-wise Optimization

- 1: **Input:** The sample covariance matrix $\widehat{\Sigma}_{\mathbf{y}} = \frac{1}{M} \mathbf{Y} \mathbf{Y}^H$ of the $L \times M$ matrix of samples \mathbf{Y} .
 - 2: **Input:** The LSFCs of K_{tot} users $(g_1, \dots, g_{K_{\text{tot}}})$ if available.
 - 3: **Initialize:** $\Sigma = \sigma^2 \mathbf{I}_L$, $\gamma = \mathbf{0}$.
 - 4: **for** $i = 1, 2, \dots$ **do**
 - 5: Select an index $k \in [K_{\text{tot}}]$ corresponding to the k -th component of $\gamma = (\gamma_1, \dots, \gamma_{K_{\text{tot}}})^T$ randomly or according to a specific schedule.
 - 6: **ML:** Set $d_0^* = \max \left\{ \frac{\mathbf{a}_k^H \Sigma^{-1} \widehat{\Sigma}_{\mathbf{y}} \Sigma^{-1} \mathbf{a}_k - \mathbf{a}_k^H \Sigma^{-1} \mathbf{a}_k}{(\mathbf{a}_k^H \Sigma^{-1} \mathbf{a}_k)^2}, -\gamma_k \right\}$.
 - 7: **NNLS:** Set $d_0^* = \max \left\{ \frac{\mathbf{a}_k^H (\widehat{\Sigma}_{\mathbf{y}} - \Sigma) \mathbf{a}_k}{\|\mathbf{a}_k\|_2^4}, -\gamma_k \right\}$.
 - 8: Set $d^* = \min\{d_0^*, g_k - \gamma_k\}$ if LSFC g_k is available and $d^* = d_0^*$ otherwise.
 - 9: Update $\gamma_k \leftarrow \gamma_k + d^*$.
 - 10: Update $\Sigma^{-1} \leftarrow \Sigma^{-1} - \frac{d^* \Sigma^{-1} \mathbf{a}_k \mathbf{a}_k^H \Sigma^{-1}}{1 + d^* \mathbf{a}_k^H \Sigma^{-1} \mathbf{a}_k}$
 - 11: **end for**
 - 12: **Output:** The resulting estimate γ .
-

communication system. We define $\widehat{\mathcal{A}}_c(\nu) := \{i : \gamma_i^* > \nu \sigma^2\}$, with $\nu > 0$, as the estimate of the set of active users. We also define the misdetection and false-alarm probabilities as

$$P_{\text{md}}(\nu) = 1 - \frac{\mathbb{E}[|\mathcal{K}_a \cap \widehat{\mathcal{A}}_c|]}{K_a}, \quad P_{\text{fa}}(\nu) = \frac{\mathbb{E}[|\widehat{\mathcal{A}}_c \setminus \mathcal{K}_a|]}{K_{\text{tot}} - K_a} \quad (35)$$

where K_a and K_{tot} denote the number of active and the number of potential users, respectively. By varying $\nu \in \mathbb{R}_+$, we get the *Receiver Operating Characteristic* (ROC) [37] of the algorithms. For simplicity of comparison, in the results presented here we have restricted to the point of the ROC where $P_{\text{md}}(\nu) = P_{\text{fa}}(\nu)$.

We consider several models for the distribution of the LSFCs g_k . The simplest case is when all LSFCs are constant, $g_k \equiv 1$, this corresponds to a scenario with perfect power control. We also consider the case of variable signal strengths such that $10 \log_{10}(g_k)$ is randomly distributed uniformly in some range $[10 \log_{10}(g_{\min}), 10 \log_{10}(g_{\max})]$ (uniform distribution in dB scale). This corresponds to the case of partial power control, where users partially compensate for their physical pathloss and reach some target SNR out of a set of possible values. In practice, these prefixed target SNR values corresponds to the various Modulation and Coding Schemes (MCS) of a given communication protocol, which in turn correspond to different data transmission rates (see for example the MCS modes of standards such as IEEE 802.11 [38] or 3GPP-LTE [4]). In passing, we notice here the importance of estimating not only the user activity pattern but their LSFCs, in order to perform rate allocation. Such a distribution, for specific values of g_{\min} and g_{\max} was also considered in [11].

B. MMV-AMP

This version of AMP, as introduced in [39], is a Bayesian iterative recovery algorithm for the MMV problem, i.e., it aims to recover an unknown matrix with i.i.d. rows from linear Gaussian measurements. As said in the introduction, the use of MMV-AMP has been proposed in [11, 14] for the AD problem in a Bayesian setting, where the LSFCs are either known, or its distribution is known. Since unfortunately the formulation of MMV-AMP is often lacking details and certain terms (e.g., derivatives of matrix-valued functions with matrix arguments) are left indicated without explanations, for the sake of clarity and in order to provide a self-contained exposition we briefly review this algorithm here in the notation of this paper.

We can rewrite the received signal as

$$\mathbf{Y} = \mathbf{A}\mathbf{X} + \mathbf{Z} \quad (36)$$

with $\mathbf{X} = \mathbf{G}\mathbf{B}\mathbf{H}$. Let $\mathbf{X}_{k,:}$ denote the k -th row of \mathbf{X} . Letting $\lambda = \frac{K_a}{K_{\text{tot}}}$ be the fraction of active users, in the Bayesian setting underlying the MMV-AMP algorithm it is assumed that the rows of \mathbf{X} are mutually statistically independent and identically distributed according to

$$p_X(\mathbf{x}) = (1 - \lambda)\delta_0 + \lambda \int_0^{+\infty} \frac{e^{-\frac{\|\mathbf{x}\|_2^2}{\zeta}}}{\pi\zeta} dp_G(\zeta), \quad (37)$$

where $p_G(\cdot)$ is the distribution of the LSFCs, i.e., for each k , it is assumed that $\mathbf{X}_{k,:}$ is either the identically zero vector (with probability λ) or a conditionally complex i.i.d. M -dim Gaussian vector with mean 0 and conditional variance g_k . Furthermore, the g_k 's are i.i.d. $\sim p_G(\cdot)$. The conditional distribution of $\mathbf{X}_{k,:}$ given g_k is obviously given by

$$p_{X|g}(\mathbf{x}|g_k) = (1 - \lambda)\delta_0 + \lambda \frac{e^{-\frac{\|\mathbf{x}\|_2^2}{g_k}}}{\pi g_k}. \quad (38)$$

The MMV-AMP iteration is defined as follows:

$$\mathbf{X}^{t+1} = \eta_t(\mathbf{A}^H \mathbf{Z}^t + \mathbf{X}^t) \quad (39)$$

$$\mathbf{Z}^{t+1} = \mathbf{Y} - \mathbf{A}\mathbf{X}^{t+1} + \frac{K_{\text{tot}}}{L} \mathbf{Z}^t \langle \eta_t'(\mathbf{A}^H \mathbf{Z}^t + \mathbf{X}^t) \rangle \quad (40)$$

with $\mathbf{X}^0 = \mathbf{0}$ and $\mathbf{Z}^0 = \mathbf{Y}$. The function $\eta_t : \mathbb{C}^{K_{\text{tot}} \times M} \rightarrow \mathbb{C}^{K_{\text{tot}} \times M}$ is defined row-wise as

$$\eta_t(\mathbf{R}) = \begin{bmatrix} \eta_{t,1}(\mathbf{R}_{1,:}) \\ \vdots \\ \eta_{t,K_{\text{tot}}}(\mathbf{R}_{K_{\text{tot}},:}) \end{bmatrix}, \quad (41)$$

where each row function $\eta_{t,k} : \mathbb{C}^M \rightarrow \mathbb{C}^M$ is chosen as the posterior mean estimate of the random vector \mathbf{x} , with a priori distribution as the rows of \mathbf{X} as given above, in the *decoupled* Gaussian observation model

$$\mathbf{r} = \mathbf{x} + \mathbf{z}, \quad (42)$$

where \mathbf{z} is an i.i.d. complex Gaussian vector with components $\sim \mathcal{CN}(0, \Sigma_t)$. When \mathbf{g} is known, such posterior mean estimate is conditional on the knowledge of g_k , i.e., we define

$$\eta_{t,k}(\mathbf{r}) = \tilde{\eta}_t(\mathbf{r}, g_k) := \mathbb{E}[\mathbf{x}|\mathbf{r}, g_k]. \quad (43)$$

If \mathbf{g} is not known, the posterior mean estimate is unconditional, i.e., we define (with some abuse of notation)

$$\eta_{t,k}(\mathbf{r}) = \tilde{\eta}_t(\mathbf{r}) := \mathbb{E}[\mathbf{x}|\mathbf{r}]. \quad (44)$$

Notice that in the latter case $\eta_{t,k}(\cdot)$ does not depend on k , i.e., the same mapping $\tilde{\eta}_t(\cdot)$ is applied to all the rows in (41). The noise variance in the decoupled observation model, Σ_t is provided at each iteration t the following recursive equation termed *State Evolution* (SE), given by

$$\Sigma_{t+1} = \sigma^2 \mathbf{I}_M + \frac{K_{\text{tot}}}{L} \mathbb{E}[\mathbf{e}_t \mathbf{e}_t^H] \quad (45)$$

where

$$\mathbf{e}_t = \begin{cases} (\tilde{\eta}_t(\mathbf{x} + \mathbf{z}, g_k) - \mathbf{x})^\top & \text{if } \mathbf{g} \text{ is known} \\ (\tilde{\eta}_t(\mathbf{x} + \mathbf{z}) - \mathbf{x})^\top & \text{if } \mathbf{g} \text{ is not known} \end{cases} \quad (46)$$

The initial value of the SE is given by $\Sigma_0 = \sigma^2 \mathbf{I}_M + \frac{K_{\text{tot}}}{L} \mathbb{E}[\mathbf{x}\mathbf{x}^H]$. The SE equation has the important property that it can predicts the estimation error of the AMP output $\{\mathbf{X}^t\}_{t=0,1,\dots}$ asymptotically in the sense that [40]

$$\lim_{K_{\text{tot}} \rightarrow \infty} \frac{\|\mathbf{X}^{t+1} - \mathbf{X}\|_F^2}{K_{\text{tot}}} = \text{tr}(\mathbb{E}[\mathbf{e}_t \mathbf{e}_t^H]) = \text{tr}(\Sigma_t - \sigma^2 \mathbf{I}_M) \frac{L}{K_{\text{tot}}}. \quad (47)$$

Formally this was proven for the case when the entries of \mathbf{A} are Gaussian iid. In practice this property holds also when the columns of \mathbf{A} are sampled uniformly from the sphere, as in our case.

Since there is no spatial correlation between the receive antennas, Σ_0 is diagonal and it can be shown (see [14]) that Σ_t is diagonal for all t . In the case of \mathbf{g} is known to the AD estimator, a simple calculation yields the function $\tilde{\eta}_{t,k}(\mathbf{r})$ defined in (43) in the form

$$\tilde{\eta}_{t,k}(\mathbf{r}) = \phi_{t,k}(\mathbf{r}) g_k (g_k \mathbf{I}_M + \Sigma_t)^{-1} \mathbf{r}, \quad (48)$$

where the coefficient $\phi_{t,k}(\mathbf{r}) \in [0, 1]$ is the posterior mean estimate of the k -th component b_k of the activity pattern \mathbf{b} , when rewriting the decoupled observation model (42) as $\mathbf{r} = \sqrt{g_k} b_k \mathbf{h} + \mathbf{z}$. In particular, we have (details are omitted and can be found in [14])

$$\begin{aligned} \phi_{t,k}(\mathbf{r}) &= \mathbb{E}[b_k | \mathbf{r}, g_k] \\ &= p(b_k = 1 | \mathbf{r}, g_k) \\ &= \left(1 + \frac{1 - \lambda}{\lambda} \prod_{i=1}^M \left(\frac{g_k \exp\left(-\frac{g_k |r_i|^2}{\tau_{t,i}^2 (g_k + \tau_{t,i}^2)}\right)}{g_k + \tau_{t,i}^2} \right) \right)^{-1} \end{aligned} \quad (49)$$

The term $\langle \eta'(\cdot) \rangle$ in (40) is defined as

$$\langle \eta'_t(\mathbf{R}) \rangle = \frac{1}{K_{\text{tot}}} \sum_{k=1}^{K_{\text{tot}}} \eta'_{t,k}(\mathbf{R}_{k,:}), \quad (50)$$

where $\eta'_{t,k}(\cdot) \in \mathbb{C}^{M \times M}$ is the Jacobi matrix of the function $\eta_{t,k}(\cdot)$ evaluated at the k -th row $\mathbf{R}_{k,:}$ of the matrix argument \mathbf{R} . For known LSFCs and uncorrelated antennas (yielding diagonal $\Sigma_t = \text{diag}(\tau_{t,1}^2, \dots, \tau_{t,M}^2)$ for all t), the derivative is explicitly given by

$$\eta'_{t,k}(\mathbf{r}) = \phi_{t,k}(\mathbf{r}) \text{diag}(\Xi_{t,k}\mathbf{r}) + (\Xi_{t,k}\mathbf{r})(\tilde{\Xi}_{t,k}\mathbf{r})^H (\phi_{t,k}(\mathbf{r}) - \phi_{t,k}(\mathbf{r})^2) \quad (51)$$

where we define $\Xi_{t,k} = \text{diag}\left(\frac{g_k}{g_k + \tau_{t,i}^2} : i \in [M]\right)$ and $\tilde{\Xi}_{t,k} = \text{diag}\left(\frac{g_k}{\tau_{t,i}(g_k + \tau_{t,i}^2)} : i \in [M]\right)$. Analogous expressions for the case where the LSFCs g are unknown to the receiver can be found, but their expression cannot be generally given in a compact form and in general depends on the LSFC distribution $p_G(\cdot)$ (see [14] for more details).

1) MMV-AMP Scaling

For the single measurement vector (SMV) case ($M = 1$) it was shown in [40] that in the asymptotic limit $L, K_{\text{tot}}, K_a \rightarrow \infty$ with fixed ratios L/K_{tot} and K_a/K_{tot} the estimate $\mathbf{A}^H \mathbf{z}^t + \mathbf{x}^t$ in the AMP algorithm in the t -th iteration is indeed distributed like the true target signal in Gaussian noise with noise variance Σ^t given by the SE. A generalized version of this statement that includes the MMV case was proven in [41]. It was shown in [11] that, based on the state evolution equation (45), the error of activity detection vanishes in the limit $M \rightarrow \infty$ for any number of active users. It is important to notice that, in this type of SE-based analysis, first the limit $K_a, L \rightarrow \infty$ is taken at fixed M and then the limit $M \rightarrow \infty$ is taken. This makes it impossible to derive a scaling relation between M and K_a . Furthermore, this order of taking limits assumes that K_a is much larger than M . Hence, this type of analysis does not generally describe the case when M scales proportional to K_a or even a bit faster. Finally, it is implicit in this type of analysis that L, K_a and K_{tot} are asymptotically in linear relation, i.e., $\frac{K_a}{L} \rightarrow \alpha$ and $\frac{K_{\text{tot}}}{L} \rightarrow \beta$ for some $\alpha, \beta \in (0, \infty)$. Hence again, it is impossible to capture the scaling studied in our work, where K_a is essentially quadratic in L , K_{tot} can be much larger than K_a , and M scales to infinity slightly faster than K_a .

The above observation is a possible explanation for the behavior described in Section IV-B4, which is in fact quite different from what is predicted by the SE and in fact reveals an annoying non-convergent behavior of MMV-AMP when M is large with respect to L and the dimensions are of “practical interest”, i.e., not extremely large.

2) Approximations

Instead of pre-computing the sequence $(\Sigma_t)_{t=0,1,\dots}$, in the SMV case, where Σ_t reduces to a single parameter τ_t^2 , it is common to use the norm of the residual $\|\mathbf{Z}_t\|_2^2/K_{\text{tot}}$ as an empirical estimate of Σ_t [42, 43], since it leads to faster convergence [44] while disposing the need of pre-computing the state evolution recursion. We find empirically that, analogous to the SMV case, estimating the i -th diagonal entry of $\Sigma_t = \text{diag}(\tau_{t,1}^2, \dots, \tau_{t,M}^2)$ as $\tau_{t,i}^2 = \|\mathbf{Z}_{:,i}^t\|_2^2/K_{\text{tot}}$ (i.e., the empirical variance of the i -th column of the matrix \mathbf{Z}^t in (40)) leads to a good performance.

Another possible approximation arises from the observation that in the derivative (51), the diagonal terms are typically much larger than the off-diagonal terms, which is to be expected, since in expectation the off-diagonal entries of the term $(\Xi_{t,k}\mathbf{r})(\tilde{\Xi}_{t,k}\mathbf{r})^H$ vanish. So we find empirically that reducing the calculation of the derivative to just the diagonal entries, barely alters the performance in a large parameter regime, while significantly reducing the complexity of the MMV-AMP iterations from $\mathcal{O}(M^2)$ to $\mathcal{O}(M)$.

3) Activity detection with MMV-AMP

For known LSFCs an estimate of the activity pattern can be obtained directly by thresholding the posterior mean estimate of b_k (49). For statistically known LSFCs we have to calculate the integral of (49) over the distribution of the LSFCs. For large M this integral may become numerically unstable, in that case we can also use the following method: Let \mathbf{X}^{t_0} and \mathbf{Z}^{t_0} denote the output of the MMV-AMP algorithm at the final iteration. Let $\mathbf{R}^{t_0} := \mathbf{A}^H \mathbf{Z}^{t_0} + \mathbf{X}^{t_0}$. Under the assumption that the asymptotic decoupling phenomenon described in Section IV-B1 holds, i.e. that the decoupled observation model represents faithfully the statistics of the rows of \mathbf{R}^{t_0} , each row $\mathbf{R}_{k,:}^{t_0}$ is distributed as $\sqrt{\gamma_k} \mathbf{h}_k + \mathbf{z}_k$ with $\mathbf{z}_k \sim \mathcal{CN}(0, \Sigma^{t_0})$ and \mathbf{h}_k has the statistics of the Gaussian MIMO i.i.d. channel vector of user k . Furthermore we assume that Σ^{t_0} is diagonal, with entries $\tau_{t_0,i}^2 : i = 1, \dots, M$, which are estimated as described in the previous section. Then the ML estimate of γ_k from \mathbf{R}^{t_0} is given by

$$\hat{\gamma}_k = \max \left(0, \frac{\|\mathbf{R}_{k,:}^{t_0}\|_2^2}{M} - \frac{\sum_{i=1}^M \tau_{t_0,i}^2}{M} \right). \quad (52)$$

Then, the activity pattern as well as the active LSFC pattern can be obtained by thresholding the $\hat{\gamma}_k$.

4) Instability of MMV-AMP

In simulations, we have observed that the MMV-AMP algorithm as described in section IV-B, for certain parameter settings, exhibits an annoying non-convergent behavior that occurs at random with some non-negligible probability (according to the realization of the random pilot matrix \mathbf{A} , the random channel matrix \mathbf{H} , and the random observation noise). We find that this behavior occurs most frequently for either small $K_a \ll L$ and M similar to or larger than K_a , or for $M > K_a > L$. Also the dynamic range of the

LSFCs plays an important role. While this behavior occurs less frequently or completely vanishes for a small dynamic range or constant LSFCs, it occurs more frequently for large dynamic ranges. For example if we let g_k be distributed uniformly in dB scale between 0 and 20dB, known at the receiver, for $K_a = 20$ the algorithm is stable for $M = 4$, in the sense that the effective noise variance τ_t^2 decreases consistently, but unstable for $M = 10$, i.e. for many instances the actual measured values of $\|\mathbf{X}^t - \mathbf{X}\|_F^2 / (MK_{\text{tot}})$ diverge a lot from their SE prediction (45). This behavior is illustrated in Figure 1, where $\|\mathbf{X}^t - \mathbf{X}\|_F^2 / (MK_{\text{tot}})$ is plotted for $t = 1, 2, \dots$ for several samples along with τ_t^2 / M , where $\Sigma_t = \tau_t^2 \mathbf{I}_M$ is calculated according to the SE (45). For $K_a < L$ one may argue that this is an artificial behavior, which can be circumvented by simply discarding the information from some of the antennas, but this is certainly not possible for $K_a > L$, where $M > K_a$ measurements are necessary. We find that specifically in this regime $M > K_a > L$ the MMV-AMP performance differs significantly from its state evolution prediction, which is consistent with what was argued in section IV-B1. These outliers occur even if none of the approximations mentioned in section IV-B2 are applied. Although we find that approximating the derivative $\eta'(\cdot)$ as described in section IV-B2 helps to reduce the number of samples that do not converge to the state evolution prediction. Another observation is that the use of normalized pilots ($\|\mathbf{a}_k\|_2^2 = L$) improves the convergence to the SE prediction compared to Gaussian iid pilots.

C. Complexity Comparison

The complexity of the proposed covariance-based AD algorithms (ML and NNLS) scales with the size of the covariance matrix, i.e. $\mathcal{O}(L^2)$, plus the complexity of once calculating the empirical covariance matrix which is linear in ML .

The complexity of MMV-AMP in each iteration scales like $\mathcal{O}(M^2 L K_{\text{tot}})$ or, with a sub-sampled FFT matrix as pilot matrix, like $\mathcal{O}(M^2 K_{\text{tot}} \log K_{\text{tot}})$. Using the simplified derivative as described in paragraph IV-B2 the complexity is reduced to $\min(\mathcal{O}(M K_{\text{tot}} \log K_{\text{tot}}), \mathcal{O}(M K_{\text{tot}} L))$. In any case the covariance-based algorithms scale better with M and K_{tot} , while MMV-AMP scales better with L .

D. Scaling

The performance of AD is visualized in Figure 2 ('CS regime', i.e. $K_a \leq L$) and Figure 3 ($K_a > L$). Here we assumed all the LSFCs to be identically equal to 1, MMV-AMP was run with the full knowledge of the LSFCs and the ML and NNLS algorithms were run with the box-constraints described in Section III-C1. In Figure 2 the NNLS algorithm is comparably worse than MMV-AMP and ML. This is to be expected, since M is small compared to L , which leads to a significant gap between the true and the empirical covariance matrix $\|\widehat{\Sigma}_{\mathbf{y}} - \Sigma_{\mathbf{y}}\|_F$. Interestingly, although the ML algorithm is also covariance based, it still outperforms MMV-AMP. In Figure 3 we see that beyond the CS regime, the performance

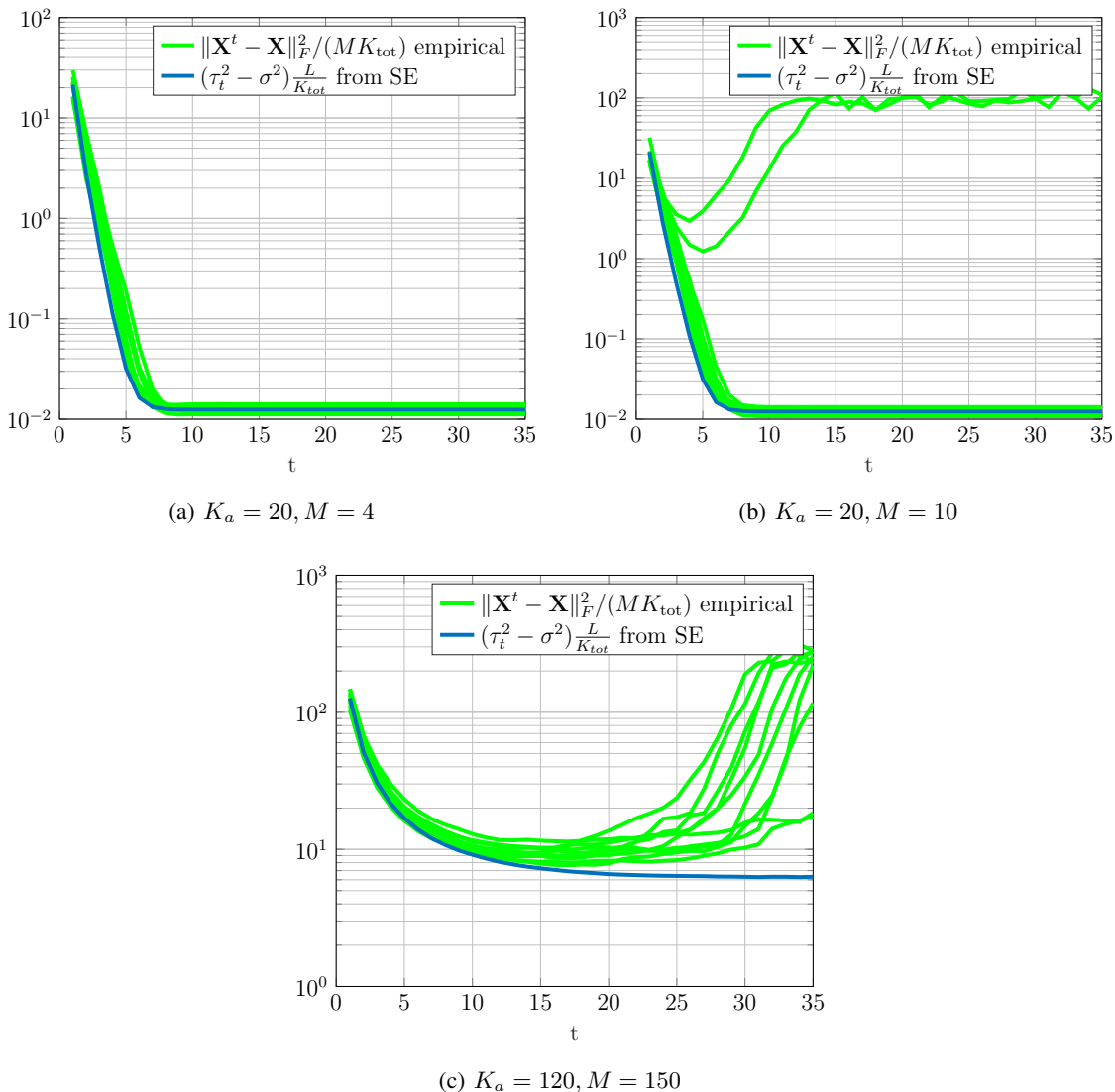


Fig. 1: Evolution of the normalized MSE in the AMP iterations (39)-(40) for 10 sample runs and its state evolution prediction from (45). $L = 100$, $K_{\text{tot}} = 2000$ and the LSFCs are chosen such that snr_k (see (3)) are uniformly distributed between 0 and 20dB and are assumed to be known at the receiver.

of MMV-AMP significantly deteriorates, while the activity detection error probability of ML and NNLS still decays exponentially with M . In Figure 4 we compare the LSFC estimation performance of the ML and NNLS algorithms. The simulations confirms Corollary 2 and show that the relative ℓ_1 recovery error of NNLS indeed decays like $1/\sqrt{M}$. We see that the same decay behavior holds for the ML algorithm only with significantly better constants.

Corollary 2 predicts that, in the limit $M \rightarrow \infty$, the recovery error of NNLS vanishes, as long as the number of active users fulfils condition (32). We confirm this behavior empirically in Figure 5a, where we solve the NNLS problem (22) using the true covariance matrix $\Sigma^\circ = \mathbf{A} \text{diag}(\gamma^\circ) \mathbf{A}^H + \sigma^2 \mathbf{I}_L$ instead of the empirical covariance matrix $\hat{\Sigma}_y$. In this case, $\|\mathbf{d}\|_2 = 0$ in (26) and the recovery error should be identically

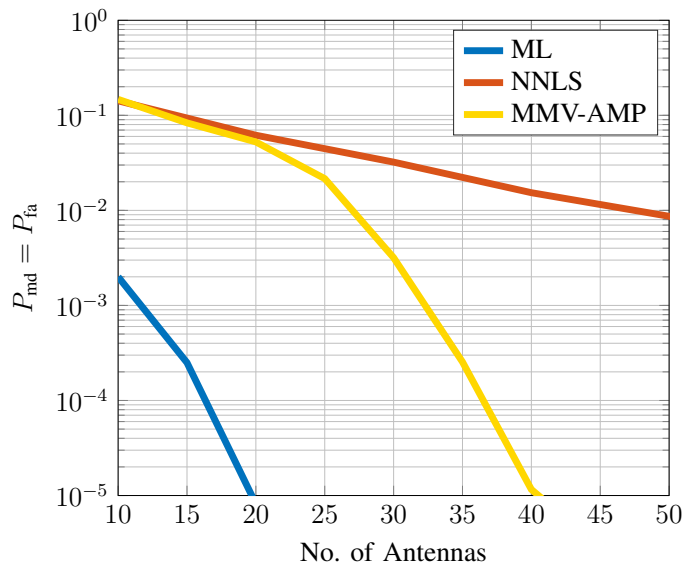


Fig. 2: Scaling of the support detection error vs. M at the border of the CS regime for $K_a = L = 100$, $K_{\text{tot}} = 2000$ with constant LSFCs at $\text{snr}_k = 0$ dB.

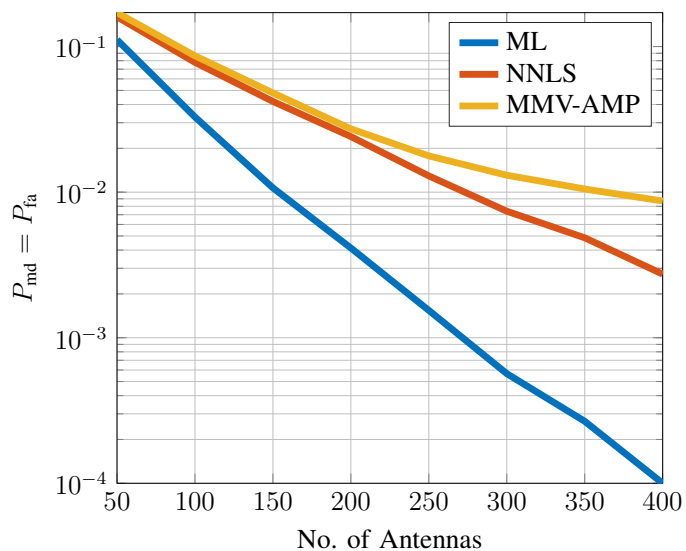


Fig. 3: Scaling of the support detection error vs. M beyond the CS regime (i.e. $K_a > L$). Here $K_a = 300$, $L = 100$, $K_{\text{tot}} = 2000$ with constant LSFCs at $\text{snr}_k = 0$ dB.

zero when the true vector γ° is K_a -sparse and the system parameters are such that Theorem 2 holds. This is confirmed by Figure 5a, showing a quadratic curve, below which the recovery error vanishes. We also observe a very similar behavior for the ML algorithm, (see Figure 5b). This suggests that the condition (22) is indeed necessary independent of the algorithm.

Figure 6 shows the gain in performance when the LSFCs are known at the receiver and the box-constraint (step 8 in Algorithm 1) is employed.

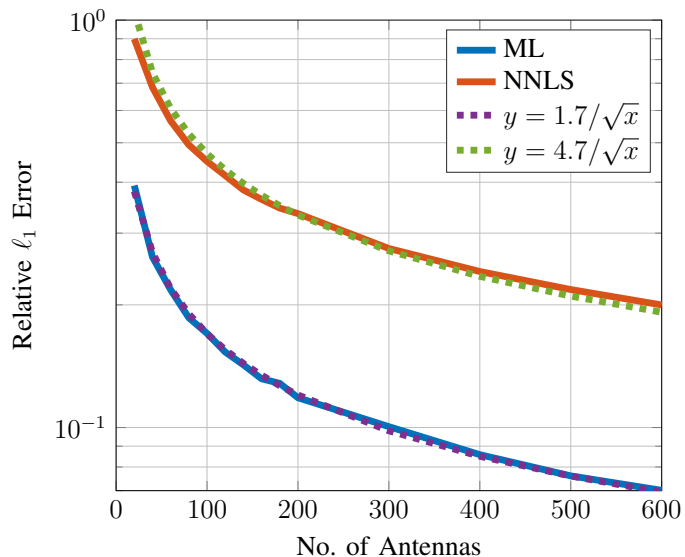


Fig. 4: Relative ℓ_1 error of the estimation of the LSFCs of the active users for $D_c = 100$, $K_a = 200$, $K_{\text{tot}} = 2000$. The LSFCs are chosen such that snr_k are uniform in the range 0-20dB. The dotted lines show that the curves are well represented by a c/\sqrt{M} behavior, for some constant c , as predicted by Corollary 2.

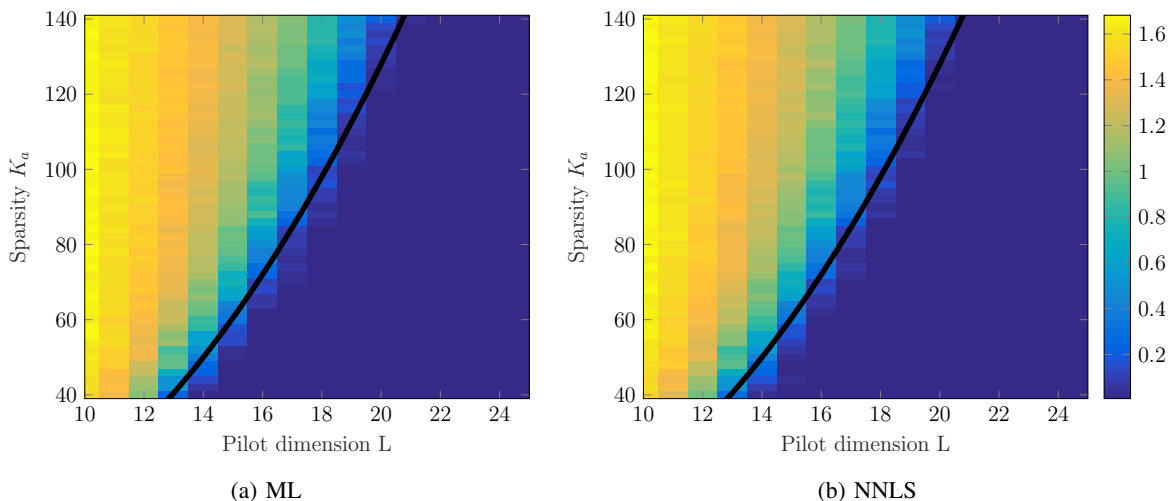


Fig. 5: Phase transition of the recovery error for NNLS and ML in the limit $M \rightarrow \infty$ for $K_{\text{tot}} = 1000$. The function $x \rightarrow (x - 4)^2/2$ is overlaid in black. The color indicates the normalized ℓ_1 -error as it is subject of Corollary 2 in the NNLS case. The LSFC are constant and the activity pattern is chosen uniformly at random from all K_a -sparse vectors. The results are obtained by averaging over random pilot matrices and activity patterns.

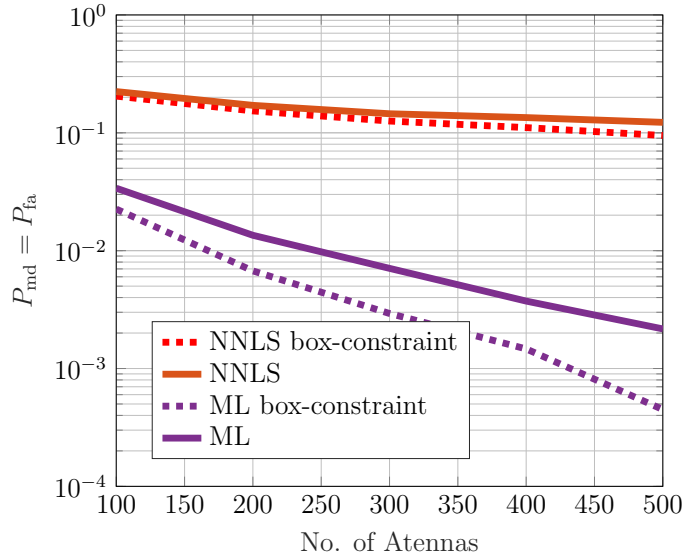


Fig. 6: Effect of using the box-constraint (see step 8 in Algorithm 1) when the LSFCs g_k are known at the receiver. Here $K_a = 150$, $L = 100$, $K_{\text{tot}} = 2000$ and the LSFCs are distributed such that snr_k are uniform in the range 0 – 20dB.

V. APPLICATION: MASSIVE MIMO UNSOURCED RANDOM ACCESS

As an application of the presented non-Bayesian algorithms and their analysis, in this section we introduce an extension of the recently posed unsourced random access problem [6] to the case of a massive MIMO BS receiver and show that the proposed ML scheme (see Algorithm 1) provides an efficient low-complexity approach. The presented scaling properties in Corollary 4 enable us to estimate the required per-user-power, in terms of E_b/N_0 , and the required number of receive antennas M for reliable transmission.

The channel model is the same as described in Section II-A, i.e., a block-fading channel with blocks of L signal dimensions over which the user channel vectors are constant. We assume $n = SL$, for some integer S , such that the transmission of a codeword spans S fading blocks. Following the problem formulation in [6], each user is given the same codebook $\mathcal{C} = \{\mathbf{c}(m) : m \in [2^{nR}]\}$, formed by 2^{nR} codewords $\mathbf{c}(m) \in \mathbb{C}^n$. An unknown number K_a of users transmits their message over the coherence block.³ The BS must then produce a list \mathcal{L} of the transmitted messages $\{m_k : k \in \mathcal{K}_a\}$ (i.e., the messages of the active users). The system performance is expressed in terms of the *Per-User Probability of Misdetection*, defined as the average fraction of transmitted messages not contained in the list, i.e.,

$$p_{md} = \frac{1}{K_a} \sum_{k \in \mathcal{K}_a} \mathbb{P}(m_k \notin \mathcal{L}), \quad (53)$$

³Here, as in [6] and in [25], we assume that users are synchronized. This assumption is not very restrictive since it is reasonable to assume that all users in the system can listen to a common reference signal.

and the *Probability of False-Alarm*, defined as the average fraction of decoded messages that were indeed not sent, i.e.,

$$p_{fa} = \frac{|\mathcal{L} \setminus \{m_k : k \in \mathcal{K}_a\}|}{|\mathcal{L}|}. \quad (54)$$

The size of the list is also an outcome of the decoding algorithm, and therefore it is a random variable. Notice that in this problem formulation the number of total users K_{tot} is completely irrelevant, as long as much larger than the range of possible active user set sizes K_a (e.g., we may consider $K_{\text{tot}} = \infty$). Letting the average energy per symbol of the codebook \mathcal{C} be denoted by $E_s = \frac{1}{n2^{nR}} \sum_{m=1}^{2^{nR}} \|\mathbf{c}(m)\|_2^2$, the received signal can be re-normalized such that the AWGN per-component variance is $\sigma^2 = N_0/E_s$ and the received energy per code symbol is 1. In this way, the notation introduced for the AD model in (1) is preserved. Furthermore, as customary in coded systems, we express energy efficiency in terms of the standard quantity $E_b/N_0 := \frac{E_s}{RN_0}$.

A. Unsourced random access as AD problem

For now assume $S = 1$, i.e. each user transmits his codeword in a single block of length L . Further fix $J = LR$ and let $\mathbf{A} \in \mathbb{C}^{L \times 2^J} = [\mathbf{a}_1, \dots, \mathbf{a}_{2^J}]$, be a matrix with columns normalized such that $\|\mathbf{a}_i\|_2^2 = L$. Each column of \mathbf{A} represents one codeword. Let i_k denote the J -bit messages produced by the active users $k \in \mathcal{K}_a$, represented as integers in $[1 : 2^J]$, user k simply sends the column \mathbf{a}_{i_k} of the coding matrix \mathbf{A} . The received signal at the M -antennas BS takes on the form

$$\begin{aligned} \mathbf{Y} &= \sum_{k \in \mathcal{K}_a} \sqrt{g_k} \mathbf{a}_{i_k} \mathbf{h}_k^\top + \mathbf{Z} \\ &= \mathbf{A} \Phi \mathbf{G}^{1/2} \mathbf{H} + \mathbf{Z} \end{aligned} \quad (55)$$

where, as for the AD model in (2), $\mathbf{G} = \text{diag}(g_1, \dots, g_{K_{\text{tot}}})$ is the diagonal matrix of LSFCs, $\mathbf{H} \in \mathbb{C}^{K_{\text{tot}} \times M}$ is the matrix containing, by rows, the user channel vectors \mathbf{h}_k formed by the small-scale fading antenna coefficients (Gaussian i.i.d. entries $\sim \mathcal{CN}(0, 1)$), $\mathbf{Z} \in \mathbb{C}^{L \times M}$ is the matrix of AWGN samples (i.i.d. entries $\sim \mathcal{CN}(0, \sigma^2)$), and $\Phi \in \{0, 1\}^{2^J \times K_{\text{tot}}}$ is a binary selection matrix where for each $k \in \mathcal{K}_a$ the corresponding column $\Phi_{:,k}$ is all-zero but a single one in position i_k , and for all $k \in \mathcal{K}_{\text{tot}} \setminus \mathcal{K}_a$ the corresponding column $\Phi_{:,k}$ contains all zeros.

Let's focus on the matrix $\mathbf{X} = \Phi \mathbf{G}^{1/2} \mathbf{H}$ of dimension $2^J \times M$. The r -th row of such matrix is given by

$$\mathbf{X}_{r,:} = \sum_{k \in \mathcal{K}_a} \sqrt{g_k} \phi_{r,k} \mathbf{h}_k^\top, \quad (56)$$

where $\phi_{r,k}$ is the (r, k) -th element of Φ , equal to one if $r = i_k$ and zero otherwise. It follows that $\mathbf{X}_{r,:}$ is Gaussian with i.i.d. entries $\sim \mathcal{CN}(0, \sum_{k \in \mathcal{K}_a} g_k \phi_{r,k})$. Since the messages are uniformly distributed over

$[1 : 2^J]$ and statistically independent across the users, the probability that $\mathbf{X}_{r,:}$ is identically zero is given by $(1 - 2^{-J})^{K_a}$. Hence, for 2^J significantly larger than K_a , the matrix \mathbf{X} is row-sparse.

In order to map the decoding into a problem completely analogous to the AD problem already discussed before, with some abuse of notation we define the modified LSFC-activity coefficients $\gamma_r := \sum_{k \in \mathcal{K}_a} g_k \phi_{r,k}$ and $\mathbf{\Gamma} = \text{diag}(\gamma_1, \dots, \gamma_{2^J})$. Then, (55) can be written as

$$\mathbf{Y} = \mathbf{A}\mathbf{\Gamma}^{1/2}\tilde{\mathbf{H}} + \mathbf{Z}, \quad (57)$$

where $\tilde{\mathbf{H}} \in \mathbb{C}^{2^J \times M}$ with i.i.d. elements $\sim \mathcal{CN}(0, 1)$. Notice that in (57) the number of total users K_{tot} plays no role. In fact, none of the matrices involved in (57) depends on K_{tot} .

The task of the inner decoder at the BS is to identify the non-zero elements of the modified active LSFC pattern γ , the vector of diagonal coefficients of $\mathbf{\Gamma}$. The active (non-zero) elements correspond to the indices of the transmitted messages. Notice that even if two or more users choose the same submessage, the corresponding modified LSFC γ_r is positive since it corresponds to the sum of the signal powers. In other words, since the detection scheme is completely non-coherent (it never explicitly estimates the complex channel matrix) and active signals add in power, there is no risk of signal cancellation or destructive interference.

At this point, it is clear that the problem of identifying the set of transmitted messages from observation (57) is completely analogous to the AD problem from the observation in (2), where the role of the total number of users K_{tot} in the AD problem is replaced by the number of messages 2^J in the inner decoding problem. Building on this analogy, we shall use our proposed ML algorithm to decode the inner code.

It is interesting to notice that the modified LSFCs in γ are random sums of the individual user channel gains $\{g_k\}$. Hence, even if the g_k 's were exactly individually known, or their statistics was known, these random sums would have unknown values and unknown statistics (unless averaging over all possible active subsets, which would involve an exponential complexity in K_{tot} which is clearly infeasible in our context). Hence, Bayesian approaches such as MMV-AMP (see Section IV-B) as advocated in [9, 11, 14, 45] do not find a straightforward application here. In contrast, the proposed non-Bayesian approaches (in particular, the ML algorithm in Algorithm 1), that treats γ as a deterministically unknown vector.

Notice also that in a practical unsourced random access scenario such as a large-scale IoT application, the slot dimension L may be of the order of 100 to 200 symbols, while for a city-wide IoT data collector it is not unreasonable to have M of the order of 500 to 1000 antennas (especially when considering narrowband signals such as in LoRA-type applications [46, 47]). This is precisely the regime where we have observed a critical behavior of MMV-AMP, while our algorithm uniformly improves as M increases, for any slot dimension L .

B. Discussion and analysis

In this section we discuss the performance of the ML decoder in a single slot ($S = 1$). For the sake of simplicity, in the discussion of this section we assume $g_k = 1$ for all k . In this case, the SNR E_s/N_0 is also the SNR at the receiver, for each individual (active) user.

Corollary 2 shows that the probability of an error in the estimation of the support of γ vanishes in the limit $M \rightarrow \infty$ for any SNR $\frac{E_s}{N_0} > 0$ as long as $K_a = \mathcal{O}(L^2/\log^2(e2^J/L^2))$. Then Corollary 2 gives the following bound for the reconstruction error of

$$\frac{\|\gamma - \gamma^*\|_1}{\|\gamma\|_1} \leq \kappa \left(1 + \left(K_a \frac{E_s}{N_0} \right)^{-1} \right) \sqrt{\frac{K_a}{M}} \quad (58)$$

where κ is some universal constant and γ^* denotes the estimate of γ by the NNLS algorithm (see section III-B). Our numerical results (section IV-D) suggest that the reconstruction error of the ML algorithm is at least as good as that of NNLS (in practice it is typically *much better*). This bound is indeed very conservative. Nevertheless, this is enough to give achievable scaling laws for the probability of error of the inner decoder. It follows from (58) that $\frac{\|\gamma - \gamma^*\|_1}{\|\gamma\|_1} \rightarrow 0$ for $(M, K_a, \frac{E_s}{N_0}) \rightarrow (\infty, \infty, 0)$ as long as

$$\frac{K_a(1 + (K_a E_s/N_0)^{-1})^2}{M} = o(1), \quad (59)$$

which is satisfied if M grows as

$$M = \max(K_a, (E_s/N_0)^{-1})^\kappa \quad (60)$$

for some $\kappa > 1$. Assuming that J scales such that $2^J = \delta L^2$ for some fixed $\delta \geq 1$, i.e. $J = \mathcal{O}(\log L)$, then the condition in Corollary 2 becomes $K_a = \mathcal{O}(L^2)$ and we can conclude that the recovery error vanishes for sum spectral efficiencies up to

$$\frac{K_a J}{L} = \mathcal{O}(L \log L). \quad (61)$$

This shows that, in principles, we can achieve a total spectral efficiency that grows without bound, by encoding over larger and larger blocks of dimension L , as long as the number of messages per user and the number of active users both grow proportionally to L^2 , when the number of BS antennas scales as in (60), this system achieves a sum spectral efficiency that grows with $L \log(L)$ and an error probability as small as desired, for any given $E_b/N_0 > 0$. Of course, in this regime the rate per active user vanishes as $\log(L)/L$.

We wish to stress again that this system is completely non-coherent, i.e., there is no attempt to either explicitly (via pilot symbols) or implicitly to estimate the channel matrix (small-scale fading coefficients).

C. Reducing complexity via concatenated coding

In practice it is not feasible to transmit even small messages (e.g. $J \sim 100$) within one coherence block ($S = 1$), because the number of columns of the coding matrix \mathbf{A} grows exponentially in J . Let each user transmit his message over a *frame* of S fading blocks and within each block use the code described in section V-A as *inner* code with the ML decoder as inner decoder.

We follow the concatenated coding scheme approach of [25], suitably adapted to our case. Let $B = nR$ denote the number of bits per user message. For some suitable integers $S \geq 1$ and $J > 0$, we divide the B -bit message into blocks of size b_1, b_2, \dots, b_S such that $\sum_s b_s = B$ and such that $b_1 = J$ and $b_s < J$ for all $s = 2, \dots, S$. Each subblock $s = 2, 3, \dots, S$ is augmented to size J by appending $p_s = J - b_s$ parity bits, obtained using pseudo-random linear combinations of the information bits of the previous blocks $s' < s$. Therefore, there is a one-to-one association between the set of all sequences of coded blocks and the paths of a tree of depth S . The pseudo-random parity-check equations generating the parity bits are identical for all users, i.e., each user makes use exactly of the same outer *tree code*. For more details on the outer coding scheme, please refer to [25].

Given J and the slot length L , the inner code is used to transmit in sequence the S (outer-encoded) blocks forming a frame. Let \mathbf{A} be the coding matrix as defined in section V-A. Each column of \mathbf{A} now represents one inner codeword. Letting $i_k(1), \dots, i_k(S)$ denote the sequence of S (outer-)encoded J -bit messages produced by the outer encoder of active user $k \in \mathcal{K}_a$. The user k now simply sends in sequence, over consecutive slots of length L , the columns $\mathbf{a}_{i_k(1)}, \mathbf{a}_{i_k(2)}, \dots, \mathbf{a}_{i_k(S)}$ of the coding matrix \mathbf{A} . As described in section V-A, the inner decoding problem is equivalent to the AD problem (57). For each subslot s , let $\hat{\boldsymbol{\gamma}}[s] = (\hat{\gamma}_1[s], \dots, \hat{\gamma}_{2^J}[s])^\top$ denote the ML estimate of $\boldsymbol{\gamma}$ in subslot s obtained by the inner decoder. Then, the list of active messages at subslot s is defined as

$$\mathcal{S}_s = \{r \in [2^J] : \hat{\gamma}_r[s] \geq \nu_s\}, \quad (62)$$

where ν_1, \dots, ν_S are suitable pre-defined thresholds. Let $\mathcal{S}_1, \mathcal{S}_2, \dots, \mathcal{S}_S$ the sequence of lists of active subblock messages. Since the subblocks contain parity bits with parity profile $\{0, p_2, \dots, p_S\}$, not all message sequences in $\mathcal{S}_1 \times \mathcal{S}_2 \times \dots \times \mathcal{S}_S$ are possible. The role of the outer decoder is to identify all possible message sequences, i.e., those corresponding to paths in the tree of the outer tree code [25]. The output list \mathcal{L} is initialized as an empty list. Starting from $s = 1$ and proceeding in order, the decoder converts the integer indices \mathcal{S}_s back to their binary representation, separates data and parity bits, computes the parity checks for all the combinations with messages from the list \mathcal{L} and extends only the paths in the tree which fulfill the parity checks. A precise analysis of the error probability of such a decoder and its complexity in terms of surviving paths in the list is given in [25]. The performance of the concatenated system is demonstrated via simulations in the following section.

D. Simulations

The outer decoder requires a hard decision on the support of the estimated $\hat{\gamma}[s]$. When K_a is known, one approach consists of selecting the $K_a + \Delta$ largest entries in each section, where $\Delta \geq 0$ can be adjusted to balance between false alarm and misdetection in the outer channel. However, the knowledge of K_a is a very restrictive assumption in such type of systems. An alternative approach, which does not require this knowledge, consists of fixing a sequence of thresholds $\{\nu_s : s \in [S]\}$ and let $\rho[s]$ to be the binary vector of dimension 2^J with elements equal to 1 for all components of $\hat{\gamma}[s]$ above threshold ν_s . By choosing the thresholds, we can balance between missed detections and false alarms. Furthermore, we may consider the use of a non-uniform decaying power allocation across the slots as described in [48].

For the simulations in Figure 7 we choose $B = 96$ bits as payload size for each user, a frame of choose $S = 32$ slots of $L = 100$ dimensions per slot, yielding an overall block length $n = 3200$. Choosing the binary subblock length $J = 12$, the inner coding matrix \mathbf{A} has dimension 100×4096 and therefore is still quite manageable. We choose the columns of \mathbf{A} uniformly i.i.d. from the sphere of radius \sqrt{L} . Notice also that if one wishes to send the same payload message using the piggybacking scheme of [9, 45], each user should make use of 2^{96} columns, which is totally impractical.

For the outer code, we choose the following parity profile $p = [0, 9, 9, \dots, 9, 12, 12, 12]$, yielding an outer coding rate $R_{out} = 0.25$ information bits per binary symbol. All large scale fading coefficients are fixed to $g_k \equiv 1$. In Figure 7 we fix $N_0 = 1$ and choose the transmit power (energy per symbol), such that $E_b/N_0 = 0$ dB and the sum of the two types of error probabilities $P_e = p_{md} + p_{fa}$, (see (53) and (54)) as a function of the number of active users for different numbers of receive antennas M . Figure 8 shows how P_e falls as a function of E_b/N_0 for different values of K_a and M . Table I summarizes the required values of E_b/N_0 to achieve a total error probability $P_e < 0.05$. Notice that this corresponds to a total spectral efficiency $\mu = \frac{12}{100} \times 0.25 \times 300 = 9$ bit per channel use, which is significantly larger than today's LTE cellular systems (in terms of bit/s/Hz per sector) and definitely much larger than IoT-driven schemes such as LoRA [46, 47]. According to the random coding bound of [6] this is impossible to achieve for the scalar Gaussian channel (only one receive antenna), even with coherent detection and roughly five times smaller spectral efficiency than here. This shows also quantitatively that the non-coherent massive MIMO channel is very attractive for unsourced random access, since it preserves the same attractive characteristics of unsourced random access as in the non-fading Gaussian model of [6] (users transmit without any pre-negotiation, and no use of pilot symbols is needed), while the total spectral efficiency can be made as large as desired simply by increasing the number of receiver antennas.

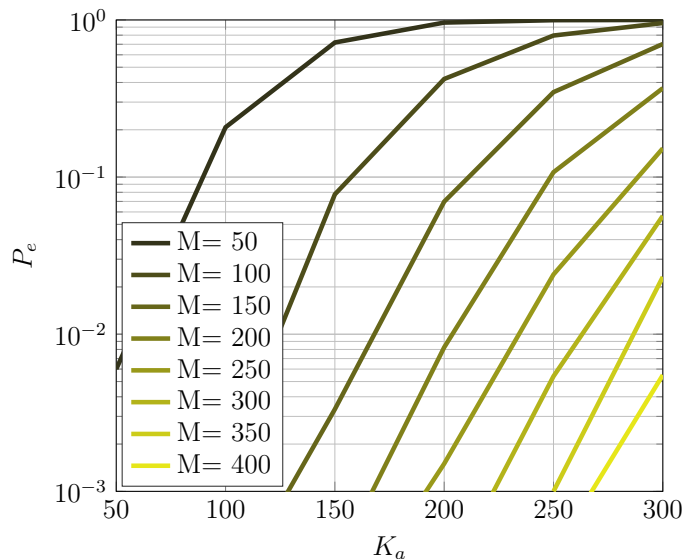


Fig. 7: Error probability ($P_e = p_{\text{md}} + p_{\text{fa}}$) as a function of the number of active users for different numbers of receive antennas. $E_b/N_0 = 0$ dB, $L = 100$, $n = 3200$, $b = 96$ bits, $S = 32$, $J = 12$.

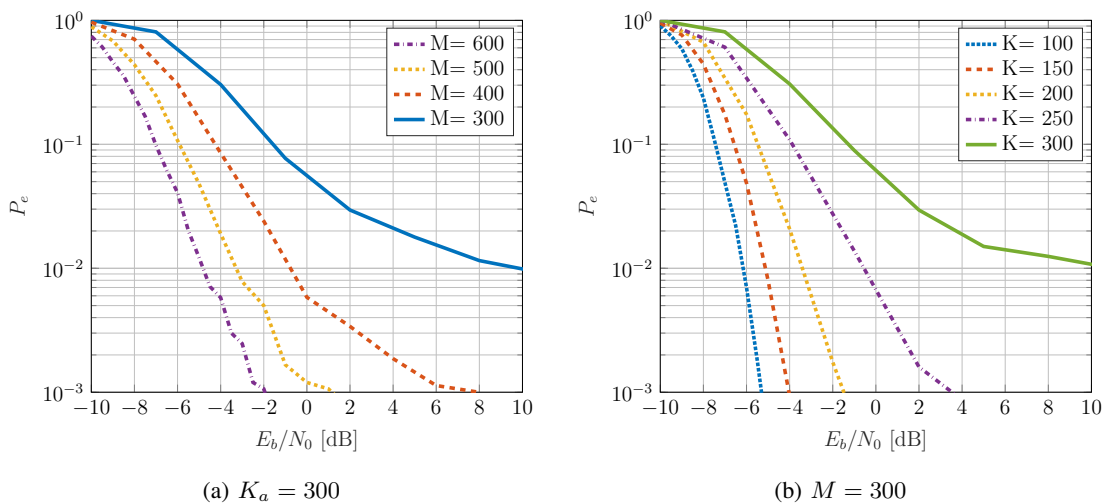


Fig. 8: Error probability ($P_e = p_{\text{md}} + p_{\text{fa}}$) as a function of E_b/N_0 . $L = 100$, $n = 3200$, $b = 96$ bits, $S = 32$, $J = 12$.

M	300	400	500	600
E_b/N_0 [dB]	0.4	-3.1	-5.0	-6.2

(a) $K_a = 300$

K_a	100	150	200	250	300
E_b/N_0 [dB]	-7.0	-6.0	-4.8	-2.9	0.6

(b) $M = 300$

TABLE I: Required E_b/N_0 to achieve a total error probability $P_e < 0.05$ with $L = 100$, $n = 3200$, $b = 96$ bits, $S = 32$, $J = 12$.

VI. CONCLUSION

In this paper, we studied the problem of user activity detection in a massive MIMO setup, where the BS has $M \gg 1$ antennas. We showed that with a coherence block containing L signal dimensions one can reliably estimate the activity of $K_a = O(L^2 / \log^2(K_{\text{tot}}/K_a))$ active users in a set of K_{tot} users, which is a much larger than the previous bound $K_a = O(L)$ obtained via traditional compressed sensing techniques. In particular, in our proposed scheme one needs to pay only a poly-logarithmic penalty $O(\log^2(K_{\text{tot}}/K_a))$ with respect to the number of potential users K_{tot} , which makes the scheme ideally suited for activity detection in IoT setups where the number of potential users can be very large. We proposed low-complexity algorithms for activity detection and provided numerical simulations to illustrate our results and compared them with approximated message passing schemes recently proposed for the same scenario. In particular, as a byproduct of our numerical investigation, we also showed a curious unstable behavior of MMV-AMP in the regime where the number of receiver antennas is large, which is precisely the case of interest with a massive MIMO receiver. Finally, we proposed a scheme for unsourced random access where all users make use of the same codebook and the receiver task is to come up with the list of transmitted messages. We use our activity detection scheme(s) directly, where now the users signature sequences play the role of codewords, and the number of total users plays the role of the number of total messages. We showed that an arbitrarily fixed probability of error can be achieved at any E_b/N_0 for sufficiently large number of antennas, and a total spectral efficiency that grows as $O(L \log L)$, where L is the code block length, can be achieved. Such one-shot scheme is conceptually nice but not suited for typical practical applications with message payload of the order of $B \approx 100$ bits, since it would require a codebook matrix with 2^B columns. Hence, we have also considered the application of the concatenated approach pioneered in [25], where the message is broken into a sequence of smaller blocks and the activity detection scheme is applied as an inner encoding/decoding stage at each block, while an outer tree code takes care of “stitching together the sequence of decoded submessages over the blocks. Numerical simulations show the effectiveness of the proposed method. It should be noticed that these schemes are completely non-coherent, i.e., the receiver never tries to estimate the massive MIMO channel matrix of complex fading coefficients. Therefore, the scheme pays no hidden penalty in terms of pilot symbol overhead, often connected with the assumption of ideal coherent reception, i.e., channel state information known to the receiver.

APPENDIX A
PROOF OF THEOREM 1

The main line of arguments in this section is based on [23]. In turns, the proof in [23] is based on a RIP result which was claimed and successively retracted [24]. The result was applied to a non-centered matrix and therefore could not have the claimed property. We fix this here, using our own new RIP result (Theorem 5) and, for the sake of clarity and self-contained presentation, give a complete streamlined proof for the case of known LSFCs. At several points our proof technique diverts from [23], which results in the slightly better bound on M . Let us first introduce some notation.

Definition 1: For $t > 1$ define the Renyi divergence of order t between two probability densities p and q as

$$\mathcal{D}_t(p, q) := \frac{1}{t-1} \ln \int p(x)^t q(x)^{1-t} dx \quad (63)$$

◇

Definition 2: A differentiable function f is called strongly convex with parameter $m > 0$ if the following inequality holds for all points x, y in its domain:

$$f(y) \geq f(x) + \nabla f(x)^\top (y - x) + \frac{m}{2} \|x - y\|_2^2 \quad (64)$$

◇

Let \mathbf{b}° denote the true activity pattern with known sparsity K_a , and \mathbf{b}^* be the output of the estimator (10). Using the union bound, we can write

$$\begin{aligned} \mathbb{P}(\mathbf{b}^* \neq \mathbf{b}^\circ) &= \mathbb{P} \left(\max_{\mathbf{b} \in \Theta_{K_a} \setminus \{\mathbf{b}^\circ\}} p(\mathbf{Y}|\mathbf{b}) \geq p(\mathbf{Y}|\mathbf{b}^\circ) \right) \\ &= \mathbb{P} \left(\bigcup_{\mathbf{b} \in \Theta_{K_a} \setminus \{\mathbf{b}^\circ\}} \{p(\mathbf{Y}|\mathbf{b}) \geq p(\mathbf{Y}|\mathbf{b}^\circ)\} \right) \\ &\leq \sum_{\mathbf{b} \in \Theta_{K_a} \setminus \{\mathbf{b}^\circ\}} \mathbb{P}(\mathbf{Y} : p(\mathbf{Y}|\mathbf{b}) - p(\mathbf{Y}|\mathbf{b}^\circ) \geq 0) \\ &\leq \sum_{\mathbf{b} \in \Theta_{K_a} \setminus \{\mathbf{b}^\circ\}} \mathbb{P}(\mathbf{Y} : p(\mathbf{Y}|\mathbf{b}) - p(\mathbf{Y}|\mathbf{b}^\circ) > -\alpha) \end{aligned} \quad (65)$$

for any $\alpha > 0$. With slight abuse of notation we define $\Sigma(\mathbf{b}) := \mathbf{A}\mathbf{B}\mathbf{G}^\circ\mathbf{A}^\mathbf{H} + \sigma\mathbf{I}_L$, the covariance matrix for a given binary pattern \mathbf{b} for a fixed vector of LSFCs \mathbf{g}° , with $\mathbf{B} = \text{diag}(\mathbf{b})$ and $\mathbf{G}^\circ = \text{diag}(\mathbf{g}^\circ)$. Let $p_{\mathbf{b}} := \mathcal{CN}(0, \Sigma(\mathbf{b}))$ denote the Gaussian distribution with covariance matrix $\Sigma(\mathbf{b})$, then $\log p(\mathbf{Y}|\mathbf{b}) = \sum_j \log p_{\mathbf{b}}(\mathbf{Y}_{:,j})$. The following large deviation property of $\log p(\mathbf{Y}|\mathbf{b})$ is established in [23, Corollary 1]:

Theorem 3:

$$\begin{aligned} & \mathbb{P} \left(\log p(\mathbf{Y}|\mathbf{b}) - \log p(\mathbf{Y}|\mathbf{b}^\circ) > -\frac{M}{2} \mathcal{D}_{1/2}(p_{\mathbf{b}}, p_{\mathbf{b}^\circ}) \right) \\ & \leq \exp \left(-\frac{M}{4} \mathcal{D}_{1/2}(p_{\mathbf{b}}, p_{\mathbf{b}^\circ}) \right) \end{aligned} \quad (66)$$

where $\mathcal{D}_{1/2}(p_{\mathbf{b}}, p_{\mathbf{b}^\circ})$ is the Renyi divergence of order 1/2 between $p_{\mathbf{b}}$ and $p_{\mathbf{b}^\circ}$ defined in Definition 1. \square

The result of Theorem 3 holds only if $\mathcal{D}_{1/2}(p_{\mathbf{b}}, p_{\mathbf{b}^\circ}) > 0$, so in the following we will establish conditions under which this is true. First, note that since $p_{\mathbf{b}}$ and $p_{\mathbf{b}^\circ}$ are zero-mean Gaussian distributions with covariance matrices $\Sigma(\mathbf{b})$ and $\Sigma(\mathbf{b}^\circ)$ resp., their Renyi divergence of order t can be expressed in closed form as:

$$\mathcal{D}_t(p_{\mathbf{b}}, p_{\mathbf{b}^\circ}) = \frac{1}{2(1-t)} \log \frac{|(1-t)\Sigma(\mathbf{b}) + t\Sigma(\mathbf{b}^\circ)|}{|\Sigma(\mathbf{b})|^{1-t} |\Sigma(\mathbf{b}^\circ)|^t} \quad (67)$$

Let $\psi(\mathbf{b}) := -\log |\Sigma(\mathbf{b})|$, then we can see that $\mathcal{D}_t(p_{\mathbf{b}}, p_{\mathbf{b}^\circ}) \geq t \frac{m^*}{4} \|\mathbf{b} - \mathbf{b}^\circ\|_2^2$, with m^* being the strong convexity constant of $\psi(\cdot)$, is equivalent to

$$\psi((1-t)\mathbf{b} + t\mathbf{b}^\circ) \leq (1-t)\psi(\mathbf{b}) + t\psi(\mathbf{b}^\circ) - \frac{1}{2} m^* t(1-t) \|\mathbf{b} - \mathbf{b}^\circ\|_2^2. \quad (68)$$

Here we used the fact that

$$\begin{aligned} \psi((1-t)\mathbf{b} + t\mathbf{b}^\circ) &= \log |\Sigma((1-t)\mathbf{b} + t\mathbf{b}^\circ)| \\ &= \log |\mathbf{A}((1-t)\mathbf{B} + t\mathbf{B}^\circ)\mathbf{G}^\circ \mathbf{A}^H + \sigma^2 \mathbf{I}_L| \\ &= \log |(1-t)\Sigma(\mathbf{b}) + t\Sigma(\mathbf{b}^\circ)| \end{aligned} \quad (69)$$

Inequality (68) is precisely the condition that $\psi(\cdot)$ is strongly convex along the line connecting \mathbf{b} and \mathbf{b}° .

So if $\psi(\cdot)$ is strongly convex on the set of $2K_a$ -sparse vectors, then

$$\mathcal{D}_t(p_{\mathbf{b}}, p_{\mathbf{b}^\circ}) \geq t \frac{m^*}{4} \|\mathbf{b} - \mathbf{b}^\circ\|_2^2 \quad (70)$$

holds for any K_a -sparse vectors \mathbf{b} and \mathbf{b}° . Let $\mathbf{b}_1, \mathbf{b}_2 \in \Theta_{K_a}$ be two arbitrary K_a -sparse vectors. Since $\log |\cdot|$ is differentiable on \mathbb{R}^+ , a Taylor expansion of $\psi(\mathbf{b}_1)$ around \mathbf{b}_2 gives:

$$\begin{aligned} \psi(\mathbf{b}_1) &= \psi(\mathbf{b}_2) + \langle \nabla \psi(\mathbf{b}_2), \mathbf{b}_1 - \mathbf{b}_2 \rangle \\ &\quad + \frac{1}{2} (\mathbf{b}_1 - \mathbf{b}_2)^\top \nabla^2 \psi(\mathbf{b}_r) (\mathbf{b}_1 - \mathbf{b}_2) \end{aligned} \quad (71)$$

for $\mathbf{b}_r = (1-r)\mathbf{b}_1 + r\mathbf{b}_2$ with some $r \in [0, 1]$. Let $\Delta \mathbf{b} := \mathbf{b}_1 - \mathbf{b}_2$, then the strong convexity of $\psi(\cdot)$ is equivalent to

$$\sum_{i,j} \frac{\partial^2 \psi}{\partial b_i \partial b_j} \Big|_{\mathbf{b}=\mathbf{b}_r} \Delta b_i \Delta b_j \geq m^* \|\mathbf{b}_1 - \mathbf{b}_2\|_2^2. \quad (72)$$

The derivatives of ψ are given by:

$$\frac{\partial \psi}{\partial b_i} \Big|_{\mathbf{b}=\mathbf{b}_r} = -\text{tr}(\Sigma(\mathbf{b}_r)^{-1} g_i^\circ \mathbf{a}_i \mathbf{a}_i^H) \quad (73)$$

$$\left. \frac{\partial \psi}{\partial b_i \partial b_j} \right|_{\mathbf{b}=\mathbf{b}_r} = \text{tr}(\boldsymbol{\Sigma}(\mathbf{b}_r)^{-1} g_i^\circ \mathbf{a}_i \mathbf{a}_i^H \boldsymbol{\Sigma}(\mathbf{b}_r)^{-1} g_j^\circ \mathbf{a}_j \mathbf{a}_j^H) \quad (74)$$

Next we will calculate m^* . It holds that

$$\begin{aligned} \sum_{i,j} \left. \frac{\partial \psi}{\partial b_i \partial b_j} \right|_{\mathbf{b}=\mathbf{b}_r} \Delta b_i \Delta b_j &= \sum_{i,j} \text{tr} \left(\boldsymbol{\Sigma}(\mathbf{b}_r)^{-1} \Delta b_i g_i^\circ \mathbf{a}_i \mathbf{a}_i^H \boldsymbol{\Sigma}(\mathbf{b}_r)^{-1} \Delta b_j g_j^\circ \mathbf{a}_j \mathbf{a}_j^H \right) \\ &= \text{tr} \left(\boldsymbol{\Sigma}(\mathbf{b}_r)^{-1} \left(\sum_i \Delta b_i g_i^\circ \mathbf{a}_i \mathbf{a}_i^H \right) \boldsymbol{\Sigma}(\mathbf{b}_r)^{-1} \left(\sum_j \Delta b_j g_j^\circ \mathbf{a}_j \mathbf{a}_j^H \right) \right) \\ &= \text{tr} \left(\boldsymbol{\Sigma}(\mathbf{b}_r)^{-1} (\boldsymbol{\Sigma}(\mathbf{b}_2) - \boldsymbol{\Sigma}(\mathbf{b}_1)) \boldsymbol{\Sigma}(\mathbf{b}_r)^{-1} (\boldsymbol{\Sigma}(\mathbf{b}_2) - \boldsymbol{\Sigma}(\mathbf{b}_1)) \right) \quad (75) \\ &\geq \sigma_{\min}(\boldsymbol{\Sigma}(\mathbf{b}_r)^{-1}) \text{tr} \left((\boldsymbol{\Sigma}(\mathbf{b}_2) - \boldsymbol{\Sigma}(\mathbf{b}_1)) \boldsymbol{\Sigma}(\mathbf{b}_r)^{-1} (\boldsymbol{\Sigma}(\mathbf{b}_2) - \boldsymbol{\Sigma}(\mathbf{b}_1)) \right) \\ &\geq \sigma_{\min}^2(\boldsymbol{\Sigma}(\mathbf{b}_r)^{-1}) \|\boldsymbol{\Sigma}(\mathbf{b}_2) - \boldsymbol{\Sigma}(\mathbf{b}_1)\|_F^2 \\ &= \frac{\|\boldsymbol{\Sigma}(\mathbf{b}_2) - \boldsymbol{\Sigma}(\mathbf{b}_1)\|_F^2}{\sigma_{\max}^2(\boldsymbol{\Sigma}(\mathbf{b}_r))}. \end{aligned}$$

Here $\sigma_{\min}(\mathbf{A})$ (resp., $\sigma_{\max}(\mathbf{A})$) denotes the minimum (resp., maximum) singular value of \mathbf{A} . In the first and the second inequality in (75) we used the fact that $\text{tr}(\mathbf{A}\mathbf{B}) \geq \sigma_{\min}(\mathbf{A})\text{tr}(\mathbf{B})$ for positive semi-definite matrices \mathbf{A}, \mathbf{B} , and in the second inequality in (75) we used the fact that the covariance matrix is symmetric and $\text{tr}(\mathbf{A}^\top \mathbf{A}) = \|\mathbf{A}\|_F^2$.

We can rewrite $\|\boldsymbol{\Sigma}(\mathbf{b}_2) - \boldsymbol{\Sigma}(\mathbf{b}_1)\|_F^2 = \|\mathbb{A}(\mathbf{g}^\circ \odot (\mathbf{b}_2 - \mathbf{b}_1))\|_2^2$, where $\mathbb{A} \in \mathbb{C}^{L^2 \times K_C}$ is the matrix defined in (23), obtained by stacking the L^2 -dim vectors $\text{vec}(\mathbf{a}_k \mathbf{a}_k^H)$ by columns. We show in (110) that $\|\mathbb{A}\mathbf{x}\|_2 \geq \|\mathring{\mathbb{A}}\mathbf{x}\|_2$ holds $\forall \mathbf{x} \in \mathbb{R}^{K_{\text{tot}}}$, with $\mathring{\mathbb{A}}$ being the centered version of \mathbb{A} , which is defined in (109).

We show in Theorem 5, that, with probability at least $1 - \exp(-C_\delta L)$, $\mathring{\mathbb{A}}/\sqrt{L(L-1)}$, the centered and rescaled version of \mathbb{A} has RIP of order $2K_a$ with constant $\delta_{2K_a} < \delta$ if condition (11) is fulfilled. In particular $\|\mathring{\mathbb{A}}\mathbf{x}\|_2^2 \geq (1 - \delta_{2K_a})L(L-1)\|\mathbf{x}\|_2^2$ holds for all $2K_a$ -sparse vectors \mathbf{x} . So the RIP of $\mathring{\mathbb{A}}$ implies that

$$\begin{aligned} \|\boldsymbol{\Sigma}(\mathbf{b}_2) - \boldsymbol{\Sigma}(\mathbf{b}_1)\|_F^2 &\geq (1 - \delta_{2K_a})L(L-1)\|\mathbf{g}^\circ \odot (\mathbf{b}_2 - \mathbf{b}_1)\|_2^2 \\ &\geq (1 - \delta_{2K_a})L(L-1)g_{\min}^2 \|\mathbf{b}_2 - \mathbf{b}_1\|_2^2 \quad (76) \\ &\geq \frac{1}{2}(1 - \delta_{2K_a})L^2 g_{\min}^2 \|\mathbf{b}_2 - \mathbf{b}_1\|_2^2 \end{aligned}$$

An upper bound on $\sigma_{\max}^2(\boldsymbol{\Sigma}(\mathbf{b}_r)) = \|\boldsymbol{\Sigma}(\mathbf{b}_r)\|_{op}^2$ can be found as follows. Note that for any binary $2K_a$ -

sparse vector \mathbf{b} , it holds that

$$\begin{aligned}
\sigma_{\max}(\Sigma(\mathbf{b})) &= \|\Sigma(\mathbf{b})\|_{op} \\
&= \left\| \sum_{k=1}^{K_{\text{tot}}} g_k^\circ b_k \mathbf{a}_k \mathbf{a}_k^H + \sigma^2 \mathbf{I} \right\|_{op} \\
&\leq g_{\max} \left\| \sum_{k \in \text{supp}(\mathbf{b})} \mathbf{a}_k \mathbf{a}_k^H \right\|_{op} + \sigma^2 \\
&= g_{\max} \left\| \sum_{k \in \text{supp}(\mathbf{b})} (\mathbf{a}_k \mathbf{a}_k^H - \mathbf{I}) + 2K_a \mathbf{I} \right\|_{op} + \sigma^2 \\
&\leq g_{\max} \left\| \sum_{k \in \text{supp}(\mathbf{b})} (\mathbf{a}_k \mathbf{a}_k^H - \mathbf{I}) \right\|_{op} + g_{\max} 2K_a + \sigma^2
\end{aligned} \tag{77}$$

Now $\sum_{k \in \text{supp}(\gamma)} (\mathbf{a}_k \mathbf{a}_k^H - \mathbf{I})$ is a sum of $2K_a$ random matrices $\mathbf{a}_k \mathbf{a}_k^H$, with \mathbf{a}_k drawn i.i.d. from the sphere of radius \sqrt{L} , and therefore sub-Gaussian.. A generic large deviation result for such matrices, e.g., the complex version of [49, Theorem 4.6.1], shows that

$$\left\| \sum_{k \in \mathcal{A}_c} (\mathbf{a}_k \mathbf{a}_k^H - \mathbf{I}) \right\|_{op} \leq \left(\sqrt{K_a} + C \left(\sqrt{L} + t \right) \right)^2 \tag{78}$$

holds with probability at least $1 - 2 \exp(-t^2)$ for some universal constant $C > 0$. Let $t = \sqrt{\beta} \max(\sqrt{K_a}, \sqrt{L})$ for some $\beta > 0$. Then (77) gives that

$$\sigma_{\max}(\Sigma(\gamma)) \leq (1 + \beta C') g_{\max} \max\{K_a, L\} + \sigma^2 \tag{79}$$

holds with probability at least $1 - \exp(-\beta \max\{K_a, L\})$ for some universal constants $c', C' > 0$. So (75) can be further bounded using (76) and (79) as

$$\frac{\|\Sigma(\mathbf{b}_2) - \Sigma(\mathbf{b}_1)\|_F^2}{\sigma_{\max}^2(\Sigma(\mathbf{b}_r))} \geq \frac{(1 - \delta_{2K_a}) g_{\min}^2 \|\mathbf{b}_2 - \mathbf{b}_1\|_2^2}{2 \left((1 + C' \beta) g_{\max} \max\left\{\frac{K_a}{L}, 1\right\} + \frac{\sigma^2}{L} \right)^2} \tag{80}$$

Together with (76) this implies that, if the pilot matrix satisfies the RIP of order $2K_a$ with constant $\delta_{2K_a} < 1$, then $\psi(\cdot)$ is strongly convex along the line between any two K_a -sparse vectors with constant

$$m^* \geq \frac{(1 - \delta_{2K_a}) g_{\min}^2}{2 \left((1 + C' \beta) g_{\max} \max\left\{\frac{K_a}{L}, 1\right\} + \frac{\sigma^2}{L} \right)^2} \tag{81}$$

with probability exceeding $1 - \exp(-\beta \max\{K_a, L\})$. Since the bound is independent of the chosen vectors and the number of $2K_a$ sparse binary vectors is bounded by $\binom{K_{\text{tot}}}{2K_a} \leq (eK_{\text{tot}}/K_a)^{2K_a} \leq (eK_{\text{tot}}/K_a)^{2 \max\{K_a, L\}}$, (81) holds in the set of *all* $2K_a$ -sparse vectors with probability exceeding

$$1 - \exp\left(-2 \max\{K_a, L\} \left(\frac{\beta}{2} - \log\left(\frac{eK_{\text{tot}}}{2K_a}\right)\right)\right) \tag{82}$$

This probability exceeds $1 - \epsilon$ if

$$\beta \geq 2 \log \left(\frac{eK_{\text{tot}}}{2K_a} \right) + \frac{\log(2/\epsilon)}{\max\{K_a, L\}} \quad (83)$$

We get that

$$m^* \geq \frac{(1 - \delta_{2K_a})g_{\min}^2}{2 \left(C' \left(2 \log \left(\frac{eK_{\text{tot}}}{2K_a} \right) + \frac{\log(2/\epsilon)}{\max\{K_a, L\}} \right) g_{\max} \max \left\{ \frac{K_a}{L}, 1 \right\} + \frac{\sigma^2}{L} \right)^2} \quad (84)$$

holds with probability exceeding $1 - \epsilon$.

Let $k_d = \|\mathbf{b}_2 - \mathbf{b}_1\|_0 \leq 2K_a$ denote the number of positions in which \mathbf{b}_2 and \mathbf{b}_1 differ, i.e. their Hamming distance. Then the Renyi divergence (70) can be lower bound as:

$$\mathcal{D}_t(p_{\mathbf{b}}, p_{\mathbf{b}^\circ}) \geq t \frac{m^*}{4} k_d \quad (85)$$

Putting everything together, we can complete the union bound. Note that there are $\binom{K_a}{k_d} \binom{K_{\text{tot}} - K_a}{k_d} \leq (3eK_{\text{tot}}K_a)^{k_d}$ ways to choose a support which differs from the true support in k_d positions. Now, denote by \mathcal{C} the event that the pilot matrix \mathbf{A} is such that the RIP condition (76) holds, and the bound (84).

Using (65), Theorem 3 and (85) we get that

$$\begin{aligned} \mathbb{P}(\mathbf{b}^* \neq \mathbf{b}^\circ, \mathcal{C}) &\leq \sum_{\mathbf{b} \in \Theta_{K_a} \setminus \{\mathbf{b}^\circ\}} \exp \left(-\frac{M}{4} \mathcal{D}_{1/2}(p_{\mathbf{b}}, p_{\mathbf{b}^\circ}) \right) \\ &\leq \sum_{k_d=1}^{2K_a} (3eK_{\text{tot}}K_a)^{k_d} \exp \left(-M \frac{m^*}{4} k_d \right) \\ &= \sum_{k_d=1}^{2K_a} \exp \left(-k_d \left(M \frac{m^*}{4} - \log(3eK_{\text{tot}}K_a) \right) \right) \end{aligned} \quad (86)$$

So let

$$M \geq \frac{4}{m^*} \log \left(3eK_{\text{tot}}K_a \frac{1+\epsilon}{\epsilon} \right) \quad (87)$$

which is precisely condition (12), then

$$\begin{aligned} \mathbb{P}(\mathbf{b}^* \neq \mathbf{b}^\circ, \mathcal{C}) &\leq \sum_{k_d=1}^{2K_a} \left(\frac{\epsilon}{1+\epsilon} \right)^{k_d} \\ &\leq \epsilon \end{aligned} \quad (88)$$

Finally

$$\begin{aligned} \mathbb{P}(\mathbf{b}^* \neq \mathbf{b}^\circ) &\leq \mathbb{P}(\mathbf{b}^* \neq \mathbf{b}^\circ, \mathcal{C}) + \mathbb{P}(\bar{\mathcal{C}}) \\ &\leq \epsilon + \epsilon + \exp(-cL) \end{aligned} \quad (89)$$

This concludes the proof of Theorem 1.

APPENDIX B

PROOF OF THE RECOVERY GUARANTEE FOR NNLS, THEOREM 2

Throughout this section let $\boldsymbol{\gamma}^*$ denote the NNLS estimate

$$\boldsymbol{\gamma}^* = \arg \min_{\boldsymbol{\gamma} \in \mathbb{R}_+^{K_{\text{tot}}}} \|\mathbb{A}\boldsymbol{\gamma} - \mathbf{w}\|_2^2 \quad (90)$$

as introduced in Section III-B, where \mathbb{A} is the $L^2 \times K_{\text{tot}}$ matrix whose k -th column is given by $\text{vec}(\mathbf{a}_k \mathbf{a}_k^H)$ and

$$\mathbf{w} = \text{vec}(\widehat{\boldsymbol{\Sigma}}_{\mathbf{y}} - \mathbf{I}_L), \quad (91)$$

where $\widehat{\boldsymbol{\Sigma}}_{\mathbf{y}}$ is assumed to be the empirical covariance matrix (5) of M iid samples from a Gaussian distribution $\mathcal{CN}(0, \boldsymbol{\Sigma}_{\mathbf{y}})$ with covariance matrix

$$\boldsymbol{\Sigma}_{\mathbf{y}} = \sum_{k=1}^{K_{\text{tot}}} \gamma_k^\circ \mathbf{a}_k \mathbf{a}_k^H + \sigma^2 \mathbf{I}_L \quad (92)$$

where $\boldsymbol{\gamma}^\circ = (\gamma_1^\circ, \dots, \gamma_{K_{\text{tot}}}^\circ) \in \mathbb{R}_+^{K_{\text{tot}}}$ is the true (unknown) activity pattern. So \mathbf{w} can be expressed as

$$\mathbf{w} = \mathbb{A}\boldsymbol{\gamma}^\circ + \mathbf{d} \quad (93)$$

for $\mathbf{d} := \text{vec}(\boldsymbol{\Sigma}_{\mathbf{y}} - \widehat{\boldsymbol{\Sigma}}_{\mathbf{y}})$. Let us introduce some notation.

Definition 3 (*Robust NSP* (4.21 in [50])): $\mathbb{A} \in \mathbb{C}^{L^2 \times K_{\text{tot}}}$ is said to satisfy the robust ℓ_q NSP of order s with parameters $0 < \rho < 1$ and $\tau > 0$ if

$$\|\mathbf{v}_S\|_q \leq \frac{\rho}{s^{1-1/q}} \|\mathbf{v}_{\bar{S}}\|_1 + \tau \|\mathbb{A}\mathbf{v}\|_2 \quad \forall \mathbf{v} \in \mathbb{R}^{K_{\text{tot}}} \quad (94)$$

holds for all subsets $S \subset [K_{\text{tot}}]$ with $|S| \leq s$. The set \bar{S} denotes here the complement of S in $[K_{\text{tot}}]$.

Definition 4 (*Sub-Exponential Norm*): Let X be a real scalar random variable. Define the sub-exponential norm of X as

$$\|X\|_{\psi_1} := \inf \left\{ t > 0 : \mathbb{E} \left[\exp \left(\frac{|X|}{t} \right) \right] \leq 2 \right\}. \quad (95)$$

A well known property of sub-exponential variables is that

$$\mathbb{P}(|X| > t) \leq 2 \exp(-ct/\|X\|_{\psi_1}) \quad \forall t > 0 \quad (96)$$

for some universal constant $c > 0$.

Definition 5 (*Sub-Exponential Random Vector*): Let \mathbf{X} be a random vector in \mathbb{R}^n . \mathbf{X} is said to be sub-exponential if all its marginals are scalar sub-exponential random variables, i.e. if

$$\sup_{\mathbf{x} \in S^{n-1}} \|\langle \mathbf{X}, \mathbf{x} \rangle\|_{\psi_1} < \infty \quad (97)$$

then we define $\|\mathbf{X}\|_{\psi_1} := \sup_{\mathbf{x} \in S^{n-1}} \|\langle \mathbf{X}, \mathbf{x} \rangle\|_{\psi_1}$, where S^{n-1} is the unit sphere in \mathbb{R}^n .

Definition 6 (*Convex Concentration Property*): Let \mathbf{X} be a random vector in \mathbb{R}^n . \mathbf{X} has the convex concentration property with constant K if for every 1-Lipschitz convex function $\phi : \mathbb{R}^n \rightarrow \mathbb{R}$, we have $\mathbb{E}[|\phi(\mathbf{X})|] < \infty$ and for every $t > 0$,

$$\mathbb{P}(|\phi(\mathbf{X}) - \mathbb{E}[\phi(\mathbf{X})]| \geq t) \leq 2 \exp(-t^2/K^2) \quad (98)$$

Furthermore let the ℓ_1 -error of the best s -sparse approximation to γ° be denoted as:

$$\sigma_s(\gamma^\circ)_1 = \min_{\|\gamma\|_0 \leq s} \|\gamma^\circ - \gamma\|_1 \quad (99)$$

If γ° is assumed to actually be s -sparse, then we obviously have $\sigma_s(\gamma^\circ)_1 = 0$. The statement of Theorem 2 will be an immediate consequence of the following theorem:

Theorem 4: If $\mathbb{A} \in \mathbb{C}^{L^2 \times K_{\text{tot}}}$ has the robust ℓ_2 NSP of order s with constants $\tau > 0$ and $\rho \in (0, 1)$ and there exists a $\mathbf{t} \in \mathbb{C}^{K_{\text{tot}}}$, such that $\mathbf{1} = \mathbb{A}^H \mathbf{t}$, where $\mathbf{1} := (1, \dots, 1)^\top$. Then for $p \in [1, 2]$ the NNLS estimate γ^* in (90) satisfies

$$\|\gamma^* - \gamma^\circ\|_p \leq \frac{2C\sigma_s(\gamma^\circ)_1}{s^{1-1/p}} + \frac{2D}{s^{\frac{1}{2}-\frac{1}{p}}} \left(\tau + \frac{\|\mathbf{t}\|_2}{s^{\frac{1}{2}}} \right) \|\mathbf{d}\|_2 \quad (100)$$

with $C := \frac{(1+\rho)^2}{1-\rho}$, $D = \frac{(3+\rho)}{1-\rho}$ and $\mathbf{d} = \text{vec}(\Sigma_{\mathbf{y}} - \widehat{\Sigma}_{\mathbf{y}})$ \square

Proof: This proof is adapted from [32] to our setting. First, we will need some implications which follow from the nullspace property [50, Theorem 4.25]. Assume that \mathbb{A} satisfies the robust NSP as stated in the theorem. Then, for any $p \in [1, 2]$ and for all $\mathbf{x}, \mathbf{z} \in \mathbb{R}^{K_{\text{tot}}}$,

$$\begin{aligned} \|\mathbf{x} - \mathbf{z}\|_p &\leq \frac{C}{s^{1-1/p}} (\|\mathbf{x}\|_1 - \|\mathbf{z}\|_1 + 2\sigma_s(\mathbf{x})_1) \\ &\quad + D\tau s^{1/p-1/2} \|\mathbb{A}(\mathbf{x} - \mathbf{z})\|_2 \end{aligned} \quad (101)$$

holds, with C, D as defined in the statement of the theorem. If $\mathbf{x}, \mathbf{z} \geq 0$ are non-negative and there exists \mathbf{t} such that $\mathbf{1} = \mathbb{A}^H \mathbf{t}$ we use:

$$\begin{aligned} \|\mathbf{x}\|_1 - \|\mathbf{z}\|_1 &= \langle \mathbf{1}, \mathbf{x} - \mathbf{z} \rangle = \langle \mathbb{A}^H \mathbf{t}, \mathbf{x} - \mathbf{z} \rangle \\ &= \langle \mathbf{t}, \mathbb{A}(\mathbf{x} - \mathbf{z}) \rangle \leq \|\mathbf{t}\|_2 \|\mathbb{A}(\mathbf{x} - \mathbf{z})\|_2 \end{aligned} \quad (102)$$

where we have used Cauchy-Schwarz inequality (note that $\langle \mathbf{t}, \mathbb{A}(\mathbf{x} - \mathbf{z}) \rangle$ is real). So inequality (101) implies:

$$\|\mathbf{x} - \mathbf{z}\|_p \quad (103)$$

$$\leq \frac{2C\sigma_s(\mathbf{x})_1}{s^{1-1/p}} + \left(D\tau + \frac{C \cdot \|\mathbf{t}\|_2}{s^{1/2}} \right) \frac{\|\mathbb{A}(\mathbf{x} - \mathbf{z})\|_2}{s^{\frac{1}{2}-\frac{1}{p}}} \quad (104)$$

Now, lets take $\mathbf{y} = \mathbb{A}\mathbf{x} + \mathbf{d}$. Since $\|\mathbb{A}(\mathbf{x} - \mathbf{z})\|_2 \leq \|\mathbb{A}\mathbf{z} - \mathbf{y}\|_2 + \|\mathbf{d}\|_2$ we get for all non-negative \mathbf{z} and \mathbf{x} :

$$\|\mathbf{x} - \mathbf{z}\|_p \quad (105)$$

$$= \frac{2C\sigma_s(\mathbf{x})_1}{s^{1-1/p}} + \left(D\tau + \frac{C \cdot \|\mathbf{t}\|_2}{s^{1/2}} \right) \frac{\|\mathbb{A}\mathbf{z} - \mathbf{y}\|_2 + \|\mathbf{d}\|_2}{s^{\frac{1}{2}-\frac{1}{p}}} \quad (106)$$

Now take $\mathbf{z} = \boldsymbol{\gamma}^*$ and $\mathbf{x} = \boldsymbol{\gamma}^\circ$, then $\mathbf{y} = \mathbf{w}$ (see (91)). Since $\boldsymbol{\gamma}^\circ \in \mathbb{R}_+^{K_{\text{tot}}}$ is itself is a feasible point of the minimization we have $\min_{\boldsymbol{\gamma} \in \mathbb{R}_+^{K_{\text{tot}}}} \|\mathbb{A}\boldsymbol{\gamma} - \mathbf{b}\|_2 \leq \|\mathbf{d}\|_2$, yielding:

$$\|\boldsymbol{\gamma}^* - \boldsymbol{\gamma}^\circ\|_p \leq \frac{2C\sigma_s(\boldsymbol{\gamma}^\circ)_1}{s^{1-1/p}} + 2 \left(D\tau + \frac{C \cdot \|\mathbf{t}\|_2}{s^{1/2}} \right) \frac{\|\mathbf{d}\|_2}{s^{\frac{1}{2}-\frac{1}{p}}} \quad (107)$$

It is easily checked that $C \leq D$ for $\rho \in (0, 1)$, which gives the result. \blacksquare

In our case we choose $\mathbf{t} = t \cdot \text{vec}(\mathbf{I}_L) \in \mathbb{R}^{L^2}$ with some $t > 0$. Let \mathbb{A}_k be the k -th column of \mathbb{A} . It holds that

$$\mathbb{A}_k^H \text{vec}(\mathbf{I}_L) = \text{tr}(\mathbf{a}_k \mathbf{a}_k^H) = \|\mathbf{a}_k\|_2^2. \quad (108)$$

Using the normalization of the pilots $\|\mathbf{a}_k\|_2^2 = L$, we get that:

$$\mathbb{A}^H \mathbf{t} = tL \cdot \mathbf{1}$$

so $t = 1/L$, and therefore $\|\mathbf{t}\|_2^2 = 1/L$ gives the desired condition $\mathbb{A}^H \mathbf{t} = \mathbf{1}$. Before we can make use of Theorem 4 it remains to show that \mathbb{A} has the robust ℓ_2 -NSP with high probability. To this end, we will restrict to those measurements which are related to the isotropic part of \mathbb{A} . More precisely, define the centered version of \mathbb{A} , denoted by $\mathring{\mathbb{A}}$ as the $L(L-1) \times K_{\text{tot}}$ dimensional matrix, with the k -th column given by

$$\mathring{\mathbb{A}}_{:,k} := \text{vec}_{\text{non-diag}}(\mathbf{a}_k \mathbf{a}_k^H - \text{diag}(\mathbf{a}_k \mathbf{a}_k^H)). \quad (109)$$

Where $\text{vec}_{\text{non-diag}}(\cdot)$ denotes the vectorization of only the non-diagonal elements, which in the case of $\mathbf{a}_k \mathbf{a}_k^H - \text{diag}(\mathbf{a}_k \mathbf{a}_k^H)$, are zero anyway. Now it is easy to check (revert the vectorization) that this special structure gives us the inequality:

$$\|\mathbb{A}\mathbf{v}\|_2^2 = \|\mathring{\mathbb{A}}\mathbf{v}\|_2^2 + \|\mathbb{A}^{\text{diag}}\mathbf{v}\|_2^2 \geq \|\mathring{\mathbb{A}}\mathbf{v}\|_2^2 \quad (110)$$

where $\mathbb{A}^{\text{diag}} \in \mathbb{C}^{L \times K_{\text{tot}}}$ is defined as the non-isotropic part of \mathbb{A} with its k -th column defined by $\mathbb{A}_{:,k}^{\text{diag}} = \text{vec}(\text{diag}(\mathbf{a}_k \mathbf{a}_k^H))$. This shows that if $\mathring{\mathbb{A}}$ has the ℓ_2 -NSP of order s with constants τ and ρ , then so does \mathbb{A} , since

$$\begin{aligned} \|\mathbf{v}_S\|_2 &= \frac{\rho}{\sqrt{s}} \|\mathbf{v}_{\bar{S}}\|_1 + \tau \left\| \mathring{\mathbb{A}}\mathbf{v} \right\|_2 \\ &\leq \frac{\rho}{\sqrt{s}} \|\mathbf{v}_{\bar{S}}\|_1 + \tau \|\mathbb{A}\mathbf{v}\|_2 \end{aligned} \quad (111)$$

holds for all subsets $S \subset [K_{\text{tot}}]$ with $|S| \leq s$. It is well-known that the robust ℓ_2 -NSP of order s is implied by the restricted isometry property (RIP) of order $2s$ with sufficiently small constants [50]. More precisely,

let $m = L(L-1)$, then the restricted isometry constant $\delta_{2s} = \delta_{2s}(\mathring{\mathbf{A}}/\sqrt{m})$ of $\mathring{\mathbf{A}}/\sqrt{m}$ of order $2s$ is defined as:

$$\delta_{2s} := \sup_{0 < \|\mathbf{v}\|_0 \leq 2s} \left| \frac{\|\mathring{\mathbf{A}}\mathbf{v}\|_2^2}{m\|\mathbf{v}\|_2^2} - 1 \right| \quad (112)$$

and if $\delta_{2s} \in [0, 1)$ the matrix $\mathring{\mathbf{A}}/\sqrt{m}$ is said to have RIP of order $2s$. The normalization is necessary to ensure that the expected norm of the columns of $\mathring{\mathbf{A}}$ is of order $\mathcal{O}(1)$ for all L , which is a necessary condition for the RIP to hold with high probability. The following theorem specifies how RIP is related to the ℓ_2 -NSP

Theorem 5: If $\mathring{\mathbf{A}}$ has RIP of order $2s$ with a constant bound as $\delta_{2s}(\mathring{\mathbf{A}}/\sqrt{m}) \leq \delta < 4/\sqrt{41} \approx 0.62$ then $\mathring{\mathbf{A}}/\sqrt{m}$ has the robust ℓ_2 -NSP of order s with parameters ρ and τ' with $\rho \leq \delta/(\sqrt{1-\delta^2} - \delta/4)$ and $\tau' \leq \sqrt{1+\delta}/(\sqrt{1-\delta^2} - \delta/4)$.

Furthermore $\mathring{\mathbf{A}}$ has the robust ℓ_2 -NSP of order s with parameters ρ and $\tau = \tau'/\sqrt{m}$. \square

Proof: The first part is shown in [50, Theorem 6.13]. The last statements follows immediately from

$$\tau L \left\| \frac{1}{L} \mathring{\mathbf{A}}\mathbf{v} \right\|_2 = \tau \left\| \mathring{\mathbf{A}}\mathbf{v} \right\|_2 \quad (113)$$

■

For the RIP of $\mathring{\mathbf{A}}/\sqrt{m}$ we first establish the following results for generic matrices $\mathbf{R} \in \mathbb{R}^{m \times N}$ with independent normalized columns.

Theorem 6: Let $\mathbf{R} \in \mathbb{R}^{m \times N}$ be a matrix with independent columns $\mathbf{R}_{:,i}$, normalized such that $\|\mathbf{R}_{:,i}\|_2^2 = m$, with ψ_1 -norm at most ψ . Also assume that $N \geq m$. Then the RIP constant of \mathbf{R}/\sqrt{m} satisfies $\delta_{2s}(\mathbf{R}/\sqrt{m}) < \delta$ with probability $\geq 1 - \exp(-C'\sqrt{c_{\delta,\xi}m})$ for

$$2s = c_{\delta,\xi} \frac{m}{\log^2(eN/c_{\delta,\xi}m)}, \quad (114)$$

where $c_{\delta,\xi} \leq \min\{1, \frac{\delta^2}{(3C\xi^2)^2}\}$ for any $\xi > \psi + 1$ and $C, C' > 0$ are universal constants. \square

Proof: We make use of the following generic RIP result from [34, Theorem 3.3] for matrices with i.i.d. sub-exponential columns:

Theorem 7: Let $m \geq 1$ and s, N be integers such that $1 \leq s \leq \min(N, m)$. Let $\mathbf{R}_{:,1}, \dots, \mathbf{R}_{:,N} \in \mathbb{R}^m$ be independent sub-exponential random vectors normalized such that $\mathbb{E}[\|\mathbf{R}_{:,i}\|^2] = m$ and let $\psi = \max_{i \leq N} \|\mathbf{R}_{:,i}\|_{\psi_1}$. Let $\theta' \in (0, 1)$, $K, K' \geq 1$ and set $\xi = \psi K + K'$. Then for the matrix \mathbf{R} with columns $\mathbf{R}_{:,i}$

$$\delta_s \left(\frac{\mathbf{R}}{\sqrt{m}} \right) \leq C\xi^2 \sqrt{\frac{s}{m}} \log \left(\frac{eN}{s\sqrt{\frac{s}{m}}} \right) + \theta' \quad (115)$$

holds with probability larger than

$$1 - \exp \left(-cK\sqrt{s} \log \left(\frac{eN}{s\sqrt{\frac{s}{m}}} \right) \right) \quad (116)$$

$$- \mathbb{P} \left(\max_{i \leq N} \|\mathbf{R}_{:,i}\|_2 \geq K' \sqrt{m} \right) - \mathbb{P} \left(\max_{i \leq N} \left| \frac{\|\mathbf{R}_{:,i}\|_2^2}{m} - 1 \right| \geq \theta' \right), \quad (117)$$

where $C, c > 0$ are universal constants. \square

In order to prove Theorem 6 we shall apply Theorem 7. Let us abbreviate $\delta_s = \delta_s \left(\frac{\mathbf{R}}{\sqrt{m}} \right)$. Since $\|\mathbf{R}_{:,i}\|_2^2 = m$, the last two terms in (117) vanish for all $K' > 1$ and $\theta' > 0$. Therefore, we consider the bound

$$\delta_s \leq C\xi^2 \sqrt{\frac{s}{m}} \log \left(\frac{eN}{s\sqrt{s/m}} \right) =: D, \quad (118)$$

that holds with probability larger than

$$\mathbb{P}(\delta_s \leq D) \geq 1 - \exp \left(-cK\sqrt{s} \log \left(\frac{eN}{s\sqrt{s/m}} \right) \right) \quad (119)$$

Let $s = cm/\log^2(e\frac{N}{cm})$ for any $0 < c \leq 1$. Note that the conditions $c \leq 1$ and $N \geq m$ guarantee that $\log(e\frac{N}{cm}) \geq 1$. Plugging into (118) we see that the RIP-constant satisfies

$$\delta_s \leq C\xi^2 \sqrt{c} \frac{\log(e(\frac{N}{cm})^{3/2} \log^3(e\frac{N}{cm}))}{\log(e\frac{N}{cm})} \quad (120)$$

$$\leq C\xi^2 \sqrt{c} \left(\frac{3}{2} + \frac{3 \log \log e\frac{N}{cm}}{\log e\frac{N}{cm}} \right) \quad (121)$$

$$\leq C\xi^2 \sqrt{c} \left(\frac{3}{2} + \frac{3}{e} \right) \quad (122)$$

$$\leq 3C\xi^2 \sqrt{c} \quad (123)$$

where in the first line we made use of $m \leq N$ and in the last line we used $\log \log x / \log x \leq 1/e$. This bound fails with probability:

$$\mathbb{P}(\delta_s > D) \leq \exp \left(-\hat{c}K\sqrt{s} \log \left(e\frac{N\sqrt{m}}{s^{3/2}} \right) \right) \quad (124)$$

$$\leq \exp \left(-\hat{c}K\sqrt{s} \log \left(e\frac{N}{m} \right) \right) \quad (125)$$

$$= \exp(-\hat{c}K\sqrt{c}\sqrt{m}) \quad (126)$$

where in the second line we used $s \leq m$. The statement of Theorem 6 follows by choosing c small enough such that $\delta_s \leq \delta$. \blacksquare

We want to apply Theorem 6, which holds for real values matrices \mathbf{R} , to the matrix

$$\mathbb{A}^R := \sqrt{2}[\operatorname{Re}(\mathring{\mathbb{A}}); \operatorname{Im}(\mathring{\mathbb{A}})] \in \mathbb{R}^{2L(L-1) \times K_{\text{tot}}}, \quad (127)$$

i.e., the real matrix obtained by stacking real and imaginary part of $\mathring{\mathbb{A}}$, with $m = 2L(L-1)$ and $N = K_{\text{tot}}$.

For this we need to show that

- (i) The columns of \mathbb{A}^R are normalized to $\sqrt{2L(L-1)}$;

(ii) The columns of \mathbb{A}^R are sub-exponential with ψ_1 norm independent of the dimension.

Consider the k -th column $\mathbb{A}_{:,k}^R$ of \mathbb{A}^R . We have

$$\begin{aligned}
\|[\text{Re}(\mathring{\mathbb{A}}_{:,k}); \text{Im}(\mathring{\mathbb{A}}_{:,k})]\|_2^2 &= \|\text{Re}(\mathring{\mathbb{A}}_{:,k})\|_2^2 + \|\text{Im}(\mathring{\mathbb{A}}_{:,k})\|_2^2 \\
&= \|\mathring{\mathbb{A}}_{:,k}\|_2^2 \\
&= \sum_{i \neq j} |a_{k,i} a_{k,j}^H|^2 \\
&= \left(\sum_{i=1}^L |a_{k,i}|^2 \right)^2 - \sum_{i=1}^L |a_{k,i}|^4 \\
&= (\|\mathbf{a}_k\|_2^2)^2 - \|\mathbf{a}_k\|_2^4 \\
&= L(L-1),
\end{aligned} \tag{128}$$

where we have used the normalization of the pilot matrix \mathbf{A} . This shows (i).

For (ii) we need to show that all marginal distributions of the columns \mathbb{A}^R are sub-exponential. Note that for any vector $\mathbf{u} \in \mathbb{R}^{2L(L-1)}$ the marginal $\langle \mathbb{A}_{:,k}^R, \mathbf{u} \rangle$, can be expressed as a quadratic form in $\mathbf{a}_k^R := [\text{Re}(\mathbf{a}_k); \text{Im}(\mathbf{a}_k)]$, as the following calculation shows. Let $\mathbf{U}, \tilde{\mathbf{U}} \in \mathbb{R}^{L(L-1) \times N}$ be two matrices, such that $\mathbf{u} = [\text{vec}(\mathbf{U}), \text{vec}(\tilde{\mathbf{U}})]$. Then it holds:

$$\begin{aligned}
\left\langle \frac{\mathbb{A}_{:,k}^R}{\sqrt{2}}, \mathbf{u} \right\rangle &= \sum_{i \neq j} \left(\text{Re}(a_{ki} a_{kj}^H) \mathbf{U}_{jk} + \text{Im}(a_{ki} a_{kj}^H) \tilde{\mathbf{U}}_{jk} \right) \\
&= (\sqrt{2} \mathbf{a}_k^R)^\top \mathbf{Q}_u (\sqrt{2} \mathbf{a}_k^R)
\end{aligned} \tag{129}$$

with $\mathbf{Q}_u = \frac{1}{2} \begin{pmatrix} \mathbf{U} & \tilde{\mathbf{U}} \\ -\tilde{\mathbf{U}} & \mathbf{U} \end{pmatrix}$ and therefore $\|\mathbf{Q}_u\|_F^2 = \|\mathbf{u}\|_2^2$.

This form of \mathbf{Q}_u follows from the identities:

$$\text{Re}(a_{ki} a_{kj}) = \text{Re}(a_{ki}) \text{Re}(a_{kj}) + \text{Im}(a_{ki}) \text{Im}(a_{kj}) \tag{130}$$

$$\text{Im}(a_{ki} a_{kj}) = \text{Re}(a_{ki}) \text{Im}(a_{kj}) - \text{Im}(a_{ki}) \text{Re}(a_{kj}) \tag{131}$$

We can now use the following concentration result for quadratic forms from [51] which states that a random vector which satisfies the convex concentration property also satisfies the following inequality, known as Hanson-Wright inequality [52]:

Theorem 8 (*Theorem 2.5 in [51]*): Let \mathbf{X} be a mean zero random vector in \mathbb{R}^n , which satisfies the convex concentration property with constant B , then for any $n \times n$ matrix \mathbf{Y} and every $t > 0$,

$$\begin{aligned}
&\mathbb{P}(|\mathbf{X}^\top \mathbf{Y} \mathbf{X} - \mathbb{E}[\mathbf{X}^\top \mathbf{Y} \mathbf{X}]| > t) \\
&\leq 2 \exp \left(-c \min \left(\frac{t^2}{2B^4 \|\mathbf{Y}\|_F^2}, \frac{t}{B^2 \|\mathbf{Y}\|_{op}} \right) \right)
\end{aligned} \tag{132}$$

□.

Note that a random variable with such a mixed tail behavior is especially sub-exponential. This can be seen by bounding its moments. Let Z be a random variable with

$$\mathbb{P}(|Z| > t) \leq 2 \exp\left(-c \min\left(\frac{t^2}{B^4 \|\mathbf{Y}\|_F^2}, \frac{t}{B^2 \|\mathbf{Y}\|_{op}}\right)\right) \quad (133)$$

Since $\|\mathbf{Y}\|_{op} \leq \|\mathbf{Y}\|_F$, we have $\mathbb{P}(|Z| > t) \leq 2 \exp(-c \min(x(t)^2, x(t)))$ for $x(t) = \frac{t}{B^2 \|\mathbf{Y}\|_F}$. It follows

$$\begin{aligned} \mathbb{E}[|Z|^p] &= \int_0^\infty \mathbb{P}(|Z|^p > u) du = p \int_0^\infty \mathbb{P}(|Z| > t) t^{p-1} dt \\ &\leq 2p(B^2 \|\mathbf{Y}\|_{op})^p \left(\int_0^1 e^{-x^2} x^{p-1} dx + \int_1^\infty e^{-x} x^{p-1} dx \right) \\ &\leq 2p(B^2 \|\mathbf{Y}\|_{op})^p (\Gamma(p/2) + \Gamma(p)) \\ &\leq 4p(B^2 \|\mathbf{Y}\|_{op})^p \Gamma(p) \leq 4p(pB^2 \|\mathbf{Y}\|_{op})^p \end{aligned} \quad (134)$$

where $\Gamma(\cdot)$ is the Gamma function. So

$$(\mathbb{E}[|Z|^p])^{\frac{1}{p}} \leq cpB^2 \|\mathbf{Y}\|_{op} \quad (135)$$

which is equivalent to $\|Z\|_{\psi_1} \leq cB^2 \|\mathbf{Y}\|_{op}$ by elementary properties of sub-exponential random variables. The convex concentration property was introduced in Definition 6. In our case the pilots $\mathbf{a}_k \in \mathbb{C}^L$ are distributed uniformly on the complex L -dimensional sphere of radius L , therefore the real versions $\sqrt{2}\mathbf{a}_k^R \in \mathbb{R}^{2L}$ are distributed uniformly on the sphere of radius $2L$. A classical result states that a spherical random variable $\mathbf{X} \sim \text{Unif}(\sqrt{n}S^{n-1})$ has the even stronger (non-convex) concentration property (e.g. [49, Theorem 5.1.4]):

Theorem 9 (Concentration on the Sphere): Let $\mathbf{X} \sim \text{Unif}(\sqrt{n}S^{n-1})$ be uniformly distributed on the Euclidean sphere of radius \sqrt{n} . Then there is an universal constant $c > 0$, such that for every 1-Lipschitz function $f : \sqrt{n}S^{n-1} \rightarrow \mathbb{R}$

$$\mathbb{P}(f(\mathbf{X}) - \mathbb{E}[f(\mathbf{X})]) \leq 2 \exp(-ct^2) \quad (136)$$

□

So in particular the columns $\mathbb{A}_{:,k}^R = \sqrt{2}\mathbf{a}_k^R$ have the convex concentration property with some constant $c > 0$, independent of the dimension and it follows by (129) and Theorem 8 applied to $\mathbf{X} = \sqrt{2}\mathbf{a}_k^R$ and $\mathbf{Y} = \mathbf{Q}_{\mathbf{u}}$ that the marginals of $\langle \mathbb{A}_{:,k}^R, \mathbf{u} \rangle$ uniformly satisfy the tail bound of the Hanson-Wright inequality. As shown in (135), this implies that the columns of \mathbb{A}^R are sub-exponential with

$$\|\mathbb{A}_{:,k}^R\|_{\psi_1} = \max_{\mathbf{u} \in S^{2L(L-1)-1}} \|\langle \mathbb{A}_{:,k}^R, \mathbf{u} \rangle\|_{\psi_1} \leq C \quad (137)$$

for some universal constant $C > 0$.

With this we can apply Theorem 6.

Corollary 5: Let $\mathring{\mathbb{A}} \in \mathbb{C}^{L(L-1) \times K_{\text{tot}}}$ be the centered and isotropic version of \mathbb{A} , as defined in (109) and let $m = L(L-1)$. Then there exist universal constants $c > 0$, such that, with probability exceeding $1 - \exp(-c\delta\sqrt{m})$, it holds that $\mathring{\mathbb{A}}/\sqrt{m}$ has RIP of order $2s$ with RIP constant $\delta_{2s}(\mathring{\mathbb{A}}/\sqrt{m}) < \delta$ as long as

$$2s \leq C_\delta \frac{m}{\log^2(eK_{\text{tot}}/m)} \quad (138)$$

for some constants $c_\delta, C_\delta > 0$ depending only on δ . \square

Proof: As explained above, it follows from Theorems 6, 8 and 9 that \mathbb{A}^R , as defined in (127), has RIP of order $2s$ with RIP constant $\delta_{2s}(\mathbb{A}^R/\sqrt{2m}) < \delta$ as long as

$$2s \leq C_\delta \frac{m}{\log^2(eK_{\text{tot}}/m)}. \quad (139)$$

But it holds that

$$\left\| \frac{\mathring{\mathbb{A}}\mathbf{x}}{\sqrt{m}} \right\|_2 = \left\| \sqrt{2} \frac{[\text{Re}(\mathring{\mathbb{A}}); \text{Im}(\mathring{\mathbb{A}})]\mathbf{x}}{\sqrt{2m}} \right\|_2 = \left\| \frac{\mathbb{A}^R\mathbf{x}}{\sqrt{2m}} \right\|_2 \quad (140)$$

for any $\mathbf{x} \in \mathbb{R}^{K_{\text{tot}}}$ so $\mathring{\mathbb{A}}/\sqrt{m}$ has RIP if and only if $\mathbb{A}^R/\sqrt{2m}$ has RIP with the same constants. \blacksquare

Corollary 5 establishes the RIP of $\mathring{\mathbb{A}}/\sqrt{L(L-1)}$. If we fix $\delta < 4/\sqrt{41}$, Theorem 5 implies the robust ℓ_2 -NSP of order s for $\mathring{\mathbb{A}}$ with explicit bounds on τ and ρ . For example, $\delta = 0.5$ gives $\rho < 0.68$ and $\tau < 3/L$. As shown in (111) the robust ℓ_2 -NSP of $\mathring{\mathbb{A}}$ implies the ℓ_2 -NSP of the uncentered version \mathbb{A} of the same order with the same constants. Finally, the application of Theorem 4 concludes the proof of Theorem 2.

APPENDIX C

ANALYSIS OF ERROR OF THE SAMPLE COVARIANCE MATRIX

We first consider the simple case where $\{\mathbf{y}(t) : t \in [M]\}$, are M i.i.d. realization of a L -dim complex Gaussian vector with zero mean $\mathbb{E}[\mathbf{y}(t)] = \mathbf{0}$ and a diagonal covariance matrix $\Sigma_{\mathbf{y}} = \mathbb{E}[\mathbf{y}(t)\mathbf{y}(t)^H] = \text{diag}(\boldsymbol{\beta})$, thus, $y_i(t) \sim \mathcal{CN}(0, \beta_i)$, $i \in [L]$. Let us denote by $\Delta = \widehat{\Sigma}_{\mathbf{y}} - \Sigma_{\mathbf{y}}$ be the deviation of the sample covariance matrix from its mean. Note that the (i, j) -th component of Δ is given by

$$\Delta_{ij} = \frac{1}{M} \sum_{t \in [M]} y_i(t)y_j^*(t) - \beta_i\delta_{ij} \quad (141)$$

$$= \frac{\sqrt{\beta_i\beta_j}}{M} \sum_{t \in [M]} \left(\frac{y_i(t)}{\sqrt{\beta_i}} \frac{y_j^*(t)}{\sqrt{\beta_j}} - \delta_{ij} \right) \quad (142)$$

where $\delta_{ij} = \mathbb{1}_{\{i=j\}}$ denotes the discrete delta function. Let $Y_{ij}(t) := \frac{y_i(t)}{\sqrt{\beta_i}} \frac{y_j^*(t)}{\sqrt{\beta_j}} - \delta_{ij}$. Then

$$|\Delta_{ij}|^2 = \frac{\beta_i\beta_j}{M^2} \left| \sum_{t=1}^M Y_{ij}(t) \right|^2 \quad (143)$$

Since all $Y_{ij}(t)$ are zero mean and are independent for fixed i, j . Therefore the variance of their sum $\mathbb{E} \left[\left| \sum_{t=1}^M Y_{ij}(t) \right|^2 \right]$ is the sum of their variances. In the following we show that $\mathbb{E}[|Y_{ij}|^2] = 1$ for all i, j . For $i \neq j$, we have that

$$\begin{aligned} \mathbb{E}[|Y_{ij}|^2] &= \frac{\mathbb{E}[|y_i(t)y_j(t)^*|^2]}{\beta_i\beta_j} \\ &\stackrel{(a)}{=} \frac{\mathbb{E}[|y_i(t)|^2]}{\beta_i} \frac{\mathbb{E}[|y_j(t)|^2]}{\beta_j} \\ &= 1, \end{aligned}$$

where in (a) we used the independence of the different components of $\mathbf{y}(t)$. Also, for $i = j$, we have that

$$\begin{aligned} \mathbb{E}[|Y_{ij}|^2] &= \mathbb{E} \left[\left| \frac{|y_i(t)|^2}{\beta_i} - 1 \right|^2 \right] \\ &= \frac{\mathbb{E}[|y_i(t)|^4]}{\beta_i^2} - 2 \frac{\mathbb{E}[|y_i(t)|^2]}{\beta_i} + 1 \\ &\stackrel{(a)}{=} 2 - 2 + 1 \\ &= 1, \end{aligned} \tag{144}$$

where in (a) we used the identity $\mathbb{E}[|y_i(t)|^4] = 2\mathbb{E}[|y_i(t)|^2]^2$ for complex Gaussian random variables.

Overall, from (144) and (144), we can write $\mathbb{E}[|\Delta_{ij}|^2] = \frac{\beta_i\beta_j}{M}$. Thus, we have that

$$\begin{aligned} \mathbb{E}[\|\Delta\|_F^2] &= \sum_{ij} \mathbb{E}[|\Delta_{ij}|^2] = \frac{\sum_{i,j} \beta_i\beta_j}{M} \\ &= \frac{(\sum \beta_i)^2}{M} = \frac{\text{tr}(\Sigma_{\mathbf{y}})^2}{M}. \end{aligned} \tag{145}$$

To see how fast $\|\Delta\|_F$ concentrates around its mean, note that for fixed i, j the $Y_{ij}(t)$ are independent sub-exponential random variables with sub-exponential norm ≤ 1 (see e.g. [49, Lemma 2.7.7]). Therefore, by the elemental Bernstein inequality we can estimate that for any $\alpha > 0$

$$\begin{aligned} \mathbb{P} \left(\left| \sum_{t=1}^M Y_{ij}(t) \right| > \alpha \right) &= \mathbb{P} \left(\left| \sum_{t=1}^M Y_{ij}(t) \right| > \sqrt{\alpha} \right) \\ &\leq 2 \exp(-c \min\{\alpha/M, \sqrt{\alpha}\}) \end{aligned} \tag{146}$$

for some universal constant $c > 0$. By a union bound we can see that

$$\begin{aligned} &\mathbb{P} \left(\min_{i,j} \left| \sum_{t=1}^M Y_{ij}(t) \right| > \alpha \right) \\ &\leq \binom{L}{2} \mathbb{P} \left(\left| \sum_{t=1}^M Y_{ij}(t) \right| > \alpha \right) \\ &\leq 2 \exp(2 \log(eL) - c \min\{\alpha/M, \sqrt{\alpha}\}) \end{aligned} \tag{147}$$

By choosing α properly we can get the following statement:

Theorem 10: Let $\epsilon > 0$

$$\|\Delta\|_F \leq \frac{\text{tr}(\Sigma_{\mathbf{y}})}{\sqrt{M}} \sqrt{\frac{\log\left(\frac{2(eL)^2}{\epsilon}\right)}{c}} \quad (148)$$

holds with probability exceeding $1 - \epsilon$, if $cM > \log(2(eL)^2/\epsilon)$, where $c > 0$ is the constant in (147). \square

Proof: In (147) choose $\alpha = M\delta$ with $\delta = \log(2(eL)^2/\epsilon)/c$. Then $\min\{\alpha/M, \sqrt{\alpha}\} = \min\{\delta, \sqrt{\delta M}\}$.

Under the condition on M stated in the Theorem, $\min\{\delta, \sqrt{\delta M}\} = \delta$. So

$$\begin{aligned} & \mathbb{P}\left(\min_{i,j} \left|\sum_{t=1}^M Y_{ij}(t)\right|^2 > \delta M\right) \\ & \leq 2 \exp(2 \log(eL) - 2 \log(eL) + \log(\epsilon/2)) \\ & = \epsilon. \end{aligned} \quad (149)$$

and the statement of the Theorem follows from

$$\begin{aligned} & \mathbb{P}\left(\|\Delta\|_F > \frac{\text{tr}(\Sigma_{\mathbf{y}})}{\sqrt{M/\delta}}\right) \\ & = \mathbb{P}\left(\|\Delta\|_F^2 > \frac{\text{tr}(\Sigma_{\mathbf{y}})^2}{M/\delta}\right) \\ & = \mathbb{P}\left(\sum_{ij} \frac{\beta_i \beta_j}{M^2} \left|\sum_{t=1}^M Y_{ij}(t)\right|^2 > \frac{\text{tr}(\Sigma_{\mathbf{y}})^2}{M/\delta}\right) \\ & \leq \mathbb{P}\left(\min_{ij} \left|\sum_{t=1}^M Y_{ij}(t)\right|^2 > \delta M\right) \\ & \leq \epsilon \end{aligned} \quad (150)$$

where in the second equality we used (143) and in the last inequality we used (149). \blacksquare

Now, assume that the covariance matrix $\Sigma_{\mathbf{y}}$ is not in a diagonal form and let $\Sigma_{\mathbf{y}} = \mathbf{U} \text{diag}(\boldsymbol{\beta}) \mathbf{U}^H$ be the Singular Value Decomposition (SVD) of $\Sigma_{\mathbf{y}}$. By multiplying all the vectors $\mathbf{y}(t)$ by the orthogonal matrix \mathbf{U}^H to whiten them and noting the fact that multiplying by \mathbf{U}^H does not change the Frobenius norm of a matrix, we can see that the bound in Theorem 10, which depends on $\Sigma_{\mathbf{y}}$ only through its trace, holds true in general also for non-diagonal covariance matrices.

Remark 1: It is worthwhile to mention that although (145) was derived under the Gaussianity of the observations $\{\mathbf{y}(t) : t \in [M]\}$, the result can be easily modified for general distribution of the components of $\mathbf{y}(t)$. More specifically, let us define

$$\max_i \frac{\mathbb{E}[|y_i(t)|^4]}{\mathbb{E}[|y_i(t)|^2]^2} =: \varsigma < \infty. \quad (151)$$

Then, using (144) and applying (151) to (144), we can obtain the following upper bound

$$\mathbb{E}[\|\Delta\|_F^2] \leq \max\{\zeta - 1, 1\} \times \frac{\sum_{i,j} \beta_i \beta_j}{M} \quad (152)$$

$$\leq \max\{\zeta - 1, 1\} \times \frac{\text{tr}(\Sigma_{\mathbf{y}})^2}{M}, \quad (153)$$

which is equivalent to (145) up to the constant multiplicative factor $\max\{\zeta - 1, 1\}$. \diamond

ACKNOWLEDGEMENT

The authors would like to thank R. Kueng for inspiring discussions and helpful comments. P.J. is supported by DFG grant JU 2795/3.

REFERENCES

- [1] S. Haghghatshoar, P. Jung, and G. Caire, "Improved scaling law for activity detection in massive mimo systems," in *2018 IEEE International Symposium on Information Theory (ISIT)*, 2018.
- [2] T. Taleb and A. Kunz, "Machine type communications in 3GPP networks: Potential, challenges, and solutions," *IEEE Commun. Mag.*, vol. 50, no. 3, pp. 178–184, Mar. 2012.
- [3] M. Hasan, E. Hossain, and D. Niyato, "Random access for machine-to-machine communication in LTE-advanced networks: Issues and approaches," *IEEE Commun. Mag.*, vol. 51, no. 6, pp. 86–93, Jun. 2013.
- [4] S. Sesia, I. Toufik, and M. Baker, *LTE, The UMTS Long Term Evolution: From Theory to Practice*. Wiley Publishing, 2009.
- [5] M. Agiwal, A. Roy, and N. Saxena, "Next Generation 5G Wireless Networks: A Comprehensive Survey," *IEEE Commun. Surv. Tutor.*, vol. 18, no. 3, pp. 1617–1655, 2016.
- [6] Y. Polyanskiy, "A perspective on massive random-access," in *2017 IEEE International Symposium on Information Theory (ISIT)*, Jun. 2017, pp. 2523–2527.
- [7] C. Bockelmann, "Compressive sensing based multi-user detection for machine-to-machine communication," *Trans. on Emerging Telecommunications Technologies*, vol. 24, no. 4, pp. 389–400, 2013.
- [8] V. Boljanovic, D. Vukobratovic, P. Popovski, and C. Stefanovic, "User activity detection in massive random access: Compressed sensing vs. coded slotted aloha," *arXiv preprint arXiv:1706.09918*, 2017.
- [9] K. Senel and E. G. Larsson, "Device Activity and Embedded Information Bit Detection Using AMP in Massive MIMO," in *2017 IEEE Globecom Workshops (GC Wkshps)*, Dec. 2017.
- [10] L. Liu, E. G. Larsson, W. Yu, P. Popovski, C. Stefanovic, and E. de Carvalho, "Sparse Signal Processing for Grant-Free Massive Connectivity: A Future Paradigm for Random Access Protocols in the Internet of Things," *IEEE Signal Process. Mag.*, vol. 35, no. 5, pp. 88–99, Sep. 2018.
- [11] L. Liu and W. Yu, "Massive Connectivity With Massive MIMO - Part I: Device Activity Detection and Channel Estimation," *IEEE Transactions on Signal Processing*, vol. 66, no. 11, pp. 2933–2946, June 2018.

- [12] —, “Massive Connectivity with Massive MIMO-Part II: Achievable Rate Characterization,” *IEEE Transactions on Signal Processing*, vol. 66, no. 11, pp. 2947–2959, Jun. 2018.
- [13] D. Tse and P. Viswanath, *Fundamentals of wireless communication*. Cambridge University Press, 2005.
- [14] Z. Chen, F. Sahrabi, and W. Yu, “Sparse Activity Detection for Massive Connectivity,” *IEEE Trans. Signal Process.*, vol. 66, no. 7, pp. 1890–1904, Apr. 2018.
- [15] J. Chen and X. Huo, “Theoretical results on sparse representations of multiple-measurement vectors,” *IEEE Trans Signal Process*, pp. 4634–4643, 2006.
- [16] S. Cotter, B. Rao, Kjersti Engan, and K. Kreutz-Delgado, “Sparse solutions to linear inverse problems with multiple measurement vectors,” *IEEE Trans. Signal Process.*, vol. 53, no. 7, pp. 2477–2488, Jul. 2005.
- [17] J. M. Kim, O. K. Lee, S. Member, and J. C. Ye, “Compressive MUSIC: Revisiting the link between compressive sensing and array signal processing,” *IEEE Trans Inf. Theory*, pp. 278–301, 2012.
- [18] C. Shepard, H. Yu, N. Anand, E. Li, T. Marzetta, R. Yang, and L. Zhong, “Argos: Practical many-antenna base stations,” in *Proceedings of the 18th Annual International Conference on Mobile Computing and Networking*. ACM, 2012, pp. 53–64.
- [19] S. Malkowsky, J. Vieira, L. Liu, P. Harris, K. Nieman, N. Kundargi, I. C. Wong, F. Tufvesson, V. Öwall, and O. Edfors, “The World’s First Real-Time Testbed for Massive MIMO: Design, Implementation, and Validation,” *IEEE Access*, vol. 5, pp. 9073–9088, 2017.
- [20] N. Choubey and A. Panah, “Introducing Facebook’s new terrestrial connectivity systems Terragraph and Project ARIES,” Apr. 2016. [Online]. Available: <https://engineering.fb.com/connectivity/introducing-facebook-s-new-terrestrial-connectivity-systems-terragraph-and-project-aries/>
- [21] P. Pal and P. P. Vaidyanathan, “Pushing the Limits of Sparse Support Recovery Using Correlation Information,” *IEEE Trans. Signal Process.*, vol. 63, no. 3, pp. 711–726, Feb. 2015.
- [22] C. Wang, O. Y. Bursalioglu, H. Papadopoulos, and G. Caire, “On-the-fly large-scale channel-gain estimation for massive antenna-array base stations,” in *2016 IEEE International Conference on Communications (ICC)*, 2018.
- [23] S. Khanna and C. R. Murthy, “On the Support Recovery of Jointly Sparse Gaussian Sources using Sparse Bayesian Learning,” *arXiv:1703.04930*, Mar. 2017.
- [24] —, “Corrections to “On the Restricted Isometry of the Columnwise Khatri–Rao Product”,” *IEEE Trans. Signal Process.*, vol. 67, no. 9, pp. 2387–2388, May 2019.
- [25] V. K. Amalladinne, A. Vem, D. K. Soma, K. R. Narayanan, and J.-F. Chamberland, “A Coupled Compressive Sensing Scheme for Uncoordinated Multiple Access,” *arXiv:1809.04745*, Sep. 2018.
- [26] T. L. Marzetta and H. Yang, *Fundamentals of Massive MIMO*. Cambridge University Press, Nov. 2016.
- [27] J. Zhang, C. Wen, S. Jin, X. Gao, and K. Wong, “On Capacity of Large-Scale MIMO Multiple Access Channels with Distributed Sets of Correlated Antennas,” *IEEE J. Sel. Areas Commun.*, vol. 31, no. 2, pp. 133–148, Feb. 2013.
- [28] X. Gao, O. Edfors, F. Rusek, and F. Tufvesson, “Massive MIMO Performance Evaluation Based on Measured Propagation Data,” *IEEE Trans. Wireless Commun.*, vol. 14, no. 7, pp. 3899–3911, Jul. 2015.
- [29] J. Sherman and W. J. Morrison, “Adjustment of an inverse matrix corresponding to a change in one element of a given matrix,” *The Annals of Mathematical Statistics*, vol. 21, no. 1, pp. 124–127, 1950.
- [30] Z. Chen, F. Sahrabi, Y.-F. Liu, and W. Yu, “Covariance Based Joint Activity and Data Detection for Massive Random

- Access with Massive MIMO,” in *2019 IEEE International Conference on Communications (ICC)*, 2019.
- [31] M. Slawski and M. Hein, “Non-negative least squares for high-dimensional linear models: Consistency and sparse recovery without regularization,” *Electronic Journal of Statistics*, vol. 7, pp. 3004–3056, 2013.
- [32] R. Kueng and P. Jung, “Robust Nonnegative Sparse Recovery and the Nullspace Property of 0/1 Measurements,” *IEEE Trans. Inf. Theory*, vol. 64, pp. 689–703, 2017.
- [33] X. Song, S. Haghighatshoar, and G. Caire, “A Scalable and Statistically Robust Beam Alignment Technique for Millimeter-Wave Systems,” *IEEE Transactions on Wireless Communications*, vol. 17, no. 7, pp. 4792–4805, Jul. 2018.
- [34] R. Adamczak, A. E. Litvak, A. Pajor, and N. Tomczak-Jaegermann, “Restricted Isometry Property of Matrices with Independent Columns and Neighborly Polytopes by Random Sampling,” *Constructive Approximation*, vol. 34, no. 1, pp. 61–88, 2011.
- [35] O. Guédon, A. E. Litvak, A. Pajor, and N. Tomczak-Jaegermann, “Restricted isometry property for random matrices with heavy-tailed columns,” *Comptes Rendus Mathématique*, vol. 352, no. 5, pp. 431–434, 2014.
- [36] S. Dirksen, G. Lecu, and H. Rauhut, “On the gap between RIP-properties and sparse recovery conditions,” *arXiv:1504.05073*, Apr. 2015.
- [37] H. V. Poor, *An introduction to signal detection and estimation*. Springer Science & Business Media, 2013.
- [38] 802.11, “IEEE Standard for Information technology—Telecommunications and information exchange between systems Local and metropolitan area networks—Specific requirements - Part 11: Wireless LAN Medium Access Control (MAC) and Physical Layer (PHY) Specifications,” *IEEE Std 80211-2016 Revis. IEEE Std 80211-2012*, pp. 1–3534, Dec. 2016.
- [39] J. Kim, W. Chang, B. Jung, D. Baron, and J. C. Ye, “Belief propagation for joint sparse recovery,” *arXiv:1102.3289*, Feb. 2011.
- [40] M. Bayati and A. Montanari, “The dynamics of message passing on dense graphs, with applications to compressed sensing,” *IEEE Trans. Inf. Theory*, vol. 57, no. 2, pp. 764–785, 2011.
- [41] A. Javanmard and A. Montanari, “State evolution for general approximate message passing algorithms, with applications to spatial coupling,” *Inf Inference*, vol. 2, no. 2, pp. 115–144, Dec. 2013.
- [42] S. Rangan, “Generalized approximate message passing for estimation with random linear mixing,” *IEEE Int. Symp. Inf. Theory Proc.*, pp. 1–18, 2011.
- [43] J. Barbier and F. Krzakala, “Approximate message-passing decoder and capacity-achieving sparse superposition codes,” *IEEE Trans. Inf. Theory*, vol. 63, no. 8, pp. 1–32, 2017.
- [44] A. Greig and R. Venkataramanan, “Techniques for improving the finite length performance of sparse superposition codes,” *IEEE Trans. Commun.*, vol. 66, no. 3, pp. 905 – 917, 2018.
- [45] E. G. Larsson and R. Moosavi, “Piggybacking an Additional Lonely Bit on Linearly Coded Payload Data,” *IEEE Wirel. Commun. Lett.*, vol. 1, no. 4, pp. 292–295, Aug. 2012.
- [46] M. Centenaro, L. Vangelista, A. Zanella, and M. Zorzi, “Long-range communications in unlicensed bands: The rising stars in the IoT and smart city scenarios,” *IEEE Wirel. Commun.*, vol. 23, no. 5, pp. 60–67, Oct. 2016.
- [47] D. Bankov, E. Khorov, and A. Lyakhov, “On the Limits of LoRaWAN Channel Access,” in *2016 International Conference on Engineering and Telecommunication (EnT)*, Nov. 2016, pp. 10–14.
- [48] A. Fengler, P. Jung, and G. Caire, “SPARCs and AMP for Unsourced Random Access,” in *IEEE International Symposium on Information Theory (ISIT)*, Jul. 2019, pp. 2843–2847.

- [49] R. Vershynin, *High-Dimensional Probability: An Introduction with Applications in Data Science*, ser. Cambridge Series in Statistical and Probabilistic Mathematics. Cambridge University Press, 2018.
- [50] S. Foucart and H. Rauhut, “A mathematical introduction to compressive sensing,” *Appl. Numer. Harmon. Anal. Birkhäuser*, 2013.
- [51] R. Adamczak, “A note on the Hanson-Wright inequality for random vectors with dependencies,” *Electron. Commun. Probab.*, vol. 20, no. 72, p. 13 pp., 2015.
- [52] M. Rudelson and R. Vershynin, “Hanson-Wright inequality and sub-gaussian concentration,” *Electron. Commun. Probab.*, vol. 18, no. 82, 2013.